Holocene Climate Variability in Hispaniola: Sedimentary Alkane and Isotopic Evidence of Precipitation during the Terminal Classic Drought

A Thesis Presented for the
Master of Science
Degree
The University of Tennessee, Knoxville

Elizabeth Marie MacLennan

May 2019

Copyright © 2019 by Elizabeth Marie MacLennan
All rights reserved.

ACKNOWLEDGEMENTS

I want to thank my advisor, Dr. Sally Horn, and committee members, Dr. Kelsey Ellis and Dr. Chad Lane, for their help and support with this research project. I appreciate all of your time, energy, and knowledge that you have provided me throughout this process. The Saladilla sediment core I analyzed was recovered by Ken Orvis, Sally Horn, and Duane Cozadd with support from the National Geographic Society and the Moscoso Puello Foundation. Additional field work and radiocarbon, pollen, charcoal, and shell analyses by Maria Caffrey, Ken Orvis, and Sally Horn were funded by NGS; NSF grants #0550382, #0927619, and #0446861; Sigma Xi, and the NSF-Arizona AMS Laboratory. The isotope analyses in this research took advantage of infrastructure at the University of Tennessee and the University of North Carolina Wilmington provided by NSF grants #1657170 to Sally Horn and Matthew Kerr and #1660185 to Sally Horn, Chad Lane, and Douglas Gamble. Travel to North Carolina was funded by a grant from the Stewart K. McCroskey Memorial Fund in the Department of Geography at the University of Tennessee. I would additionally like to thank Matthew Kerr for his help with the compound-specific hydrogen isotope analysis; this research would not have been possible without it.

ABSTRACT

Laguna Saladilla (19.656 N, 71.715 W) is a large (220 ha) freshwater lake located near sea level on the north coast of Hispaniola, 2 km south of Monte Cristi National Park in the Dominican Republic, and 1 km east of the international border with Haiti. Results of prior analyses of pollen, microscopic charcoal, mollusk shells, and diatoms in an 8.5-m sediment core from the lake were interpreted to largely indicate shifts in salinity and water depth attributed to relative sea level rise over the middle and late Holocene (Caffrey et al., *Paleogeography, Paleoecology, Paleoclimatology* 436: 9–32, 2015). Mollusk assemblages indicated saline conditions at 7650 cal yr BP, when sediments contained abundant red mangrove pollen, but freshening over the late Holocene, with the lake becoming brackish at 3500 cal yr BP and transitioning ca. 2500 cal yr BP to its current freshwater condition. Increased charcoal abundance and higher percentages of Amaranthaceae pollen after 2500 cal yr BP indicate increased fires and generally dry climate in coastal north Hispaniola, but detailed climate reconstruction was not possible from the proxies examined. To develop a precipitation record for north coastal Hispaniola, I examined compound-specific hydrogen isotopes in 39 samples covering the last ca. 1700 years at Laguna Saladilla. I also analyzed hydrogen isotopes in samples of bulk sediment covering this same period. Results provided evidence of increased aridity and evapotranspiration/precipitation ratios during the time known as the Terminal Classic Drought. Results complement and extend prior proxy analyses, illustrating the benefits of hydrogen isotopes in the reconstruction of paleoenvironments. My research also tested the correlation of sedimentary bulk hydrogen to compound-specific hydrogen isotopes, showing that bulk hydrogen isotopes did not respond the same controls as the compound-specific record at this site. The correlation of bulk hydrogen isotopes to other proxies at Laguna Saladilla, however, suggest

that it is still a useful proxy for understanding past environments. This research extends upon the work of multiple studies to reconstruct climate changes during the Terminal Classic Drought in the circum-Caribbean region.

TABLE OF CONTENTS

CHAPTER I *INTRODUCTION* 1

CHAPTER II *SITE DESCRIPTION, CLIMATE HISTORY, AND PREVIOUS PROXY ANALYSES AT LAGUNA SALADILLA* 8

A. Laguna Saladilla Site Description 8
B. Climate Records from Sediment Cores from Hispaniola 9
C. Dynamics and Drivers of Caribbean Climate 16
D. ITCZ Movement in the Caribbean 20
E. Previous Proxy Analyses at Laguna Saladilla 22

CHAPTER III *STABLE ISOTOPE ANALYSIS OF CLIMATE AT LAGUNA SALADILLA* 28

A. Methods 28

i. Age Model 28
ii. Sampling 28
iii. Compound-Specific Hydrogen Isotopes 28
iv. Bulk Stable Isotopes 30
v. Comparison of Hydrogen Isotopes 32

B. Results 32

i. Bacon Age Model 32
ii. Paleoenvironmental Reconstruction 32
iii. Correlation of the Bulk and Compound-Specific Hydrogen Isotopes 35

C. Discussion 37

i. Comparison to Previous Proxy Work at Laguna Saladilla 37
ii. Comparison of Bulk and Compound-Specific Hydrogen Isotopes 39
iii. Climate Record and the Terminal Classic Drought at Laguna Saladilla 42
iv. Comparison to Other Study Sites in Hispaniola 43
v. Climate Dynamics Affecting Precipitation at Laguna Saladilla 45

CHAPTER IV *SUMMARY AND CONCLUSIONS* 47

REFERENCES 49

VITA 58

LIST OF TABLES

Table 1: Radiocarbon Dates for Laguna Saladilla 23
Table 2: Statistical Results of Correlation Between Hydrogen Isotope Results[1] 36

LIST OF FIGURES

Figure 1: Location of Laguna Saladilla on the island of Hispaniola 5
Figure 2: Laguna Saladilla age-depth model. 33

LIST OF ATTACHMENTS

Figure A.1: Proxy Diagram for Laguna Saladilla……saladillaproxydiagram.pdf

CHAPTER I

INTRODUCTION

Lacustrine sediments, collected as a profile or core, reveal an abundance of information useful to the study of past environmental conditions. The reconstruction of past environments through lake sediment comes from various indicators or proxies, such as pollen grains, microscopic and macroscopic charcoal, and stable isotopes, that provide records of past fire, vegetation, and climate. Charcoal and pollen grains are particularly useful for providing evidence of human interactions with the environment. For example, the presence of maize pollen, *Zea mays* subsp. *mays* L., indicates that humans were using the nearby land for agricultural purposes (Goman and Byrne,1998; Clement and Horn, 2001; Anchukaitis and Horn, 2005). When maize and other pollen grains from agricultural activities are associated with higher charcoal counts, one can infer that the fires were from an anthropogenic source (Clark, 1990; Whitlock and Larsen, 2001; Whitlock and Anderson, 2003). In locations known to be free from anthropogenic influence, the climate can be inferred from the vegetation that flourished in the region, as reconstructed from pollen grains. Similarly, the reconstruction of fire regimes can provide evidence of past climates, as fires require climate that allows the growth and drying of fuels. Macroscopic charcoal typically indicates fires near the study site, while microscopic charcoal can represent both nearby fires and regional fires farther from the source (Lafon et al., 2017). Together, pollen grains and charcoal from lake sediments can be useful in determining times of aridity and temperature fluctuations.

However, a limitation of using these proxies in areas known to have a history of human occupation is that it can be difficult to distinguish between climatic and anthropogenic sources of changes in the vegetation and fire record. In these areas, a more direct indicator of past

climate, such as hydrogen isotope ratios, is useful (Sachse et al., 2012). The study of the hydrogen isotopic composition of terrestrial leaf waxes in lacustrine sediment provides evidence of changes in the hydrology of a region (Sauer et al., 2001; Sachse et al., 2004; 2012; Hou et al., 2008; Douglas et al., 2012; Lane et al., 2014).

Compound-specific Hydrogen isotopic composition ($\delta^2H_{n\text{-alkanes}}$) is an important proxy for hydroclimate reconstruction as precipitation $\delta^2H_{n\text{-alkanes}}$values are mostly influenced by rainfall amount in a region (Risi et al., 2008; Douglas et al., 2012). This makes $\delta^2H_{n\text{-alkanes}}$ isotope analysis of terrestrially derived *n*-alkanes from leaf waxes a suitable proxy for evapotranspiration analysis and paleoclimate studies (Sachse et al., 2012; Lane et al., 2014). Specifically, odd-numbered long chain(>25 C atoms) *n*-alkanes($n\text{-}C_{25}$ – $n\text{-}C_{33}$) are an appropriate proxy for paleohydrology as they are generally regarded as the most reliable biomarkers for terrestrial vegetation (Schefuss et al., 2011; Douglas et al., 2012; Lane and Horn, 2013; Lane et al., 2014). In tropical environments, $\delta^2H_{n\text{-alkanes}}$values in meteoric waters are controlled primarily through the amount of precipitation (the amount effect), such that a decrease in precipitation results in increased $\delta^2H_{n\text{-alkanes}}$values (Lane et al., 2014). However, Douglas et al. (2012) found that aridity and vegetation composition were associated with $\delta^2H_{n\text{-alkanes}}$values in the tropics. Therefore, in semi-arid to arid environments in the tropics, evapotranspiration plays a large role in determining $\delta^2H_{n\text{-alkanes}}$ values. This relationship is shown by an increase in evapotranspiration correlating to an increase in $\delta^2H_{n\text{-alkanes}}$ values and $\delta^2H_{n\text{-alkanes}}$ alkanes (Douglas et al., 2012). Studying the hydrogen isotopic composition of sediments in coastal areas is especially useful as meteoric waters can be used to analyze hydrologic changes in past environments independent of the influence of sea-level changes (Schefuss et al., 2011).

An emerging proxy for past precipitation records is bulk hydrogen isotope analysis. Though still a topic of limited research, bulk sedimentary hydrogen isotopes (δ^2H_{Bulk}) values can complement the study of the $\delta^2H_{n\text{-alkanes}}$ record in lacustrine sediment. δ^2H_{Bulk} analysis focuses on the D/H ratio from bulk organic matter and these measurements can be compared to other precipitation records, such as from $\delta^2H_{n\text{-alkanes}}$ isotope studies (Krishnamurthy et al., 1995, Schimmelmann et al., 1999; Hassan and Spalding, 2001; Sauer et al., 2009; Lovan and Krishnamurthy, 2011). This type of analysis can be useful for creating a precipitation record in a location with limited alkane abundance for compound-specific isotope work.

Additionally, C/N ratios, stable carbon isotope ratios ($\delta^{13}C$), and stable nitrogen isotope ratios ($\delta^{15}N$) in lake sediments are useful geochemical proxies for interpreting sources of organic matter input and possible times of aridity. C/N ratios can be used to determine terrestrial or aquatic organic matter inputs into a lake, with a ratio from 3–9 indicating terrestrial input, 10–20 indicating mixed aquatic and terrestrial input, and 10–20 indicating aquatic input (Meybeck, 1982; Talbot, 2001; Sharpe, 2007). Higher (more positive) $\delta^{13}C$ values indicate greater input of organic matter from grasses and other herbaceous plants using the C_4 photosynthetic pathway, whereas lower (less positive) $\delta^{13}C$ values indicate higher organic input from plants using the C_3 photosynthetic pathway (Bender, 1971; Lane et al., 2004). Many herbaceous plants that use the C_4 photosynthetic pathway tend to thrive in more open and arid environments than do herbs and woody plants using the C_3 photosynthetic pathway, such that intervals in sediment cores with higher $\delta^{13}C$ values can indicate times of drought (Diefendorf et al., 2010; Kohn, 2010). Drier conditions can also make C_3 herbs more C_4-like in their isotopic signal (Diefendorf et al., 2010; Kohn, 2010). The use of these geochemical proxies can help researchers better interpret the δ^2H_{Bulk} and $\delta^2H_{n\text{-alkanes}}$ records.

For my research project, I analyzed $\delta^2H_{n\text{-alkanes}}$ isotopes and δ^2H_{Bulk}, $\delta^{13}C$, and $\delta^{15}N$ isotopes in a lake sediment core from Laguna Saladilla, on the northwestern coast of the Dominican Republic (Figure 1). The objective of my research was to expand upon previous studies of pollen, charcoal, diatoms, and shells in the sediments of Laguna Saladilla (Caffrey et al., 2015) to provide a more detailed record of the climate changes in the region. My comparison of bulk and $\delta^2H_{n\text{-alkanes}}$ isotopes also provide a test of the usefulness of δ^2H_{Bulk} isotopes, which are less commonly studied than other isotopes in the reconstruction of paleoenvironments from lake sediments.

To carry out this research, I analyzed $\delta^2H_{n\text{-alkanes}}$isotopes and δ^2H_{Bulk} isotopes from 39 stratigraphic levels in Laguna Saladilla, chosen based on the previous proxy analyses of Caffrey et al. (2015). Additionally, 15 samples were analyzed for $\delta^{13}C$ and $\delta^{15}N$ isotopes. I used these geochemical proxies to create a climate record for Laguna Saladilla spanning from ~1750 cal yr BP to present day. In addition to the creation of a precipitation record at the study site, I also present the results of the comparison of $\delta^2H_{Bulk}$and $\delta^2H_{n\text{-alkanes}}$ isotopes to better understand how to use an emerging proxy in future studies.

A detailed precipitation record from Hispaniola adds to the knowledge of the complex climate history of the Caribbean region. As Granger (1985) stated, “the climate of the Caribbean is as diverse as the number of islands within it.” The goal of this project is to better understand how different climate drivers in the Caribbean region interact with each other to influence periods of aridity and wetness, especially during more extreme periods such as the Terminal Classic Drought (Lane et al., 2014). Periods of extreme climate variations are important as they represent poorly understood, large climate shifts that had repercussions for human populations. A precipitation record from this locale of Hispaniola will be helpful to



Figure 1: Location of Laguna Saladilla on the island of Hispaniola

better understand how the multiple climate drivers of the Caribbean influence regions differently and how various regions respond to extreme events.

In this thesis research I ask the following questions:

1. What trends in precipitation are indicated by bulk and compound-specific stable hydrogen isotope data during the Terminal Classic Drought?
2. How do bulk stable hydrogen and compound-specific stable hydrogen isotope data compare to one another?
3. How do inferred changes in precipitation at Laguna Saladilla relate to changes in vegetation and fire revealed by other proxies in the same sediment core?
4. What shifts in atmospheric controls/drivers based on modern climatology could be related to any precipitation shifts identified at Laguna Saladilla, and are these drivers consistent with other hypotheses of Holocene climate change for the Caribbean region?
5. Do study results on past precipitation and climate drivers have implications for the future climate of Hispaniola?

This thesis consists of four chapters. In the following chapter, I describe the study site and the climate dynamics of the Caribbean region, provide a brief overview of the climate history and previous paleoclimate research on Hispaniola, and discuss the previous proxy analyses at the site. In chapter three, I describe the methods used and results of the stable isotope analysis, and the results, comparing them to the previous proxy work and to other sites

around Hispaniola, and explaining how the results can be used to interpret the climate history of the region. Finally, in chapter four, a brief summary of my research is presented ending with the overall conclusions of the study.

CHAPTER II

SITE DESCRIPTION, CLIMATE HISTORY, AND PREVIOUS PROXY ANALYSES AT LAGUNA SALADILLA

A. Laguna Saladilla Site Description

Laguna Saladilla (19.656 N, 71.715 W) is a 220 ha freshwater lake in Hispaniola on the northwestern coast of the Dominican Republic in the province of Monte Cristi (Figure 1). It is located ~5.3 km from the Atlantic coastline and 2 m above sea level (Caffrey et al., 2015). The province of Monte Cristi is located in the Köppen Climate Classification zone of tropical savanna (Aw), with a year-round tropical climate and an extended dry period during the summer season (Griffiths and Driscoll, 1982). Average temperature for the region is 26.5 ℃ with an average of 672 mm of rainfall per year (World Meteorological Organization, 2017). The island is characterized by tropical lowland dry forest, coastal mangrove swamps, and highland mesic and pine forests (Bolay, 1997; Caffrey, 2011).

Laguna Saladilla is underlain by Quaternary alluvial deposits (French and Schenk, 2004). The lake receives water from precipitation, seepage from adjacent wetlands, and from the Rio Masacre, which flows northward from the Cordillera Central and presently enters the lake on its southwestern side. However, satellite imagery shows that the inlet position of Rio Masacre into Laguna Saladilla may vary or can circumvent the lake altogether (Caffrey, 2011; Caffrey et al., 2015). Chemical analysis of lake water samples revealed that the water is well mixed and shows little to no anthropogenic influence, indicated by low levels of potassium and nitrate (Caffrey et al., 2015).

B. Climate Records from Sediment Cores from Hispaniola

Several lakes and wetlands on Hispaniola in addition to Laguna Saladilla have yielded sediment cores that researchers have investigated to reveal past changes in climate, vegetation, fire, and human impacts. Hodell et al. (1991) reconstructed climate for the island of Hispaniola over the last 10,500 years based on stable oxygen isotopes from ostracods in a sediment core from Lake Miragoane in the southern peninsula of Haiti. The ratio of $^{18}O/^{16}O$ ($\delta^{18}O$) in ostracods provides a proxy for the evaporation/precipitation ratio. Periods of a higher than usual $\delta^{18}O$ values indicate aridity through increased evaporation while periods with a lower $\delta^{18}O$ values indicate more humidity in the atmosphere which can be related to increased precipitation. The oxygen isotope record from Lake Miragoane presented by Hodell et al. (1991) showed the highest period of aridity in the region from 10,500–10,000 ^{14}C yr B.P., correlating with the latter part of the Younger Dryas. These findings correspond with higher percentages of shrub, Palmae, and *Podocarpus* pollen, from 10,300–8200 ^{14}C yr B.P., which indicate a drier and cooler climate (Higuera-Gundy et al., 1999). From there, conditions on Hispaniola shifted towards increased humidity from 10,000–7000 ^{14}C yr B.P., indicating higher lake levels commonly seen in the Pleistocene/Holocene transition (Hodell et al., 1991). A decline in shrub pollen occurs from 8200–5370 ^{14}C yr B.P, coinciding with an increase in pollen of Chenopodiaceae and Amaranthaceae, illustrating a shift towards increasing moisture (Higuera-Gundy et al., 1999). On Hispaniola, the wettest period appears to be from 7000–5300 ^{14}C yr B.P., during the early-middle Holocene. This period contains in the lowest $\delta^{18}O$value in the record (Hodell et al., 1991). *Trema* and *Cecropia* pollen began to dominate the sediment core from 5370–2490 ^{14}C yr B.P. and the high amounts of Moracaeae pollen from 3950–2490 ^{14}C yr B.P. provide evidence that this period was also wet (Higuera-Gundy et al., 1999). From

5200 ^{14}C yr B.P. onwards towards present day, Hispaniola experienced drier conditions. There is slightly higher evaporation from 5200–3200 ^{14}C yr B.P., continuing to higher periods of evaporation from 3200–2400 ^{14}C yr B.P. (Hodell et al., 1991). A sharp increase in evaporation and the δ^{18}O values is evident for the period 2400–1500 ^{14}C yr B.P., coinciding with a decline in mesic forest taxa (Hodell et al., 1991). This was a period of shrub expansion and an increased abundance of *Celtis* (Higuera-Gundy et al., 1999). While there was a short period of wetter conditions on the island between 1500–900 ^{14}C yr B.P., supported by high percentages of *Cecropia*, this period was followed quickly by an increase in the δ^{18}O value and evaporation continuing into the present day (Hodell et al., 1991; Higuera-Gundy et al., 1999). The presence of maize pollen from 400–180 ^{14}C yr BP was well as radiocarbon dating indicate the presence of human settlement on Hispaniola. This period is marked by an increase in *Celtis* and *Pinus*, indicating drier conditions on the island (Higuera-Gundy et al., 1999).

Hodell et al. (1991) found a strong correlation between the precipitation record and the intensity of the Milankovitch cycles, illustrated by a corresponding record of insolation differences at 10°N between August and February and the ^{18}O/^{16}O ratio. While Milankovitch cycles appear to be a major determinant of precipitation/evaporation in Hispaniola, they do not explain all the variation in the record. Furthermore, these climate trends are not seen at all locations in the Caribbean, suggesting the need for more circum-Caribbean studies to truly understand precipitation variability (Fritz et al., 2011).

Additional oxygen isotope evidence of the climate history of Hispaniola is provided by Lane et al. (2009), based on a sediment core from Laguna de Felipe on the Caribbean slope of the Cordillera Central in the Dominican Republic, spanning from ~1785 cal yr BP to the core present. The δ^{18}O from ostracod valves of fossil *C. boldii* in the dataset reach their maximum

values at ~150–100, ~450–250, ~1000–950, and ~1300–1150 cal yr BP and the minimum values occur from ~100–0, ~250–150, ~650–450, and ~1400–1300 cal yr BP. There is no significant relationship between the $\delta^{18}O$ values and the $\delta^{13}C$ values, which show a decreasing trend throughout the core over time with one positive increase around 100–50 cal yr BP. The $\delta^{18}O$ record from Laguna de Felipe is an appropriate comparison to $\delta^{2}H_{n\text{-alkanes}}$ values as a proxy for times of aridity and wet conditions as both are strongly dependent on the evaporation to precipitation or E/P ratios of the time period. As with $\delta^{2}H_{n\text{-alkanes}}$ values, a higher $\delta^{18}O$ value corresponds to drier conditions while a lower $\delta^{18}O$ value corresponds to wetter conditions.

A period of aridity documented in the $\delta^{18}O$ record at Laguna de Felipe exists from 1300–1150 cal yr BP, which aligns well with the early Terminal Classic Drought, matching records of increased charcoal in Costa Rica, decreased Ti concentrations in the Caricao Basin, and magnetic susceptibility increases in Puerto Rico as the result of high levels of Saharan African dust from increased trade winds and a southerly ITCZ placement (Horn and Sanford, 1992; Horn, 1993; Nyberg et al., 2001; Haug et al., 2003; Anchukaitis and Horn, 2005; Beets, 2006). Overall, this period of aridity during the Terminal Classic Drought appears to be related primarily to ITCZ climate dynamics, specifically a southerly displacement of the ITCZ during this time. This period of aridity continues from ~900–1000 cal yr BP corresponding to the so called "Late Phase" of the Terminal Classic Drought (Hodell et al., 2005) The $\delta^{18}O$ values then start to decrease for the period of 950–650 cal yr BP, which is indicative of decreased E/P ratios and therefore a wetter climate during this 300–year period. This period can be interpreted as a more northerly mean position of the ITCZ leading to a wetter and warmer climate, often referred to as the Medieval Climate Anomaly. The northerly position of the ITCZ during this time may have been due to a positive phase of the North Atlantic Oscillation (NAO) as well as more frequent La

Niña conditions in the Pacific Ocean, which could have induced the positive NAO phase in the Atlantic. However, seeing as currently a positive NAO phase leads to decreased precipitation across the majority of the Caribbean, it is more likely that the La Niña conditions played a more significant role in the Medieval Climate Anomaly climate (Mann et al., 2009)

Lane et al. (2011) present evidence of increased aridity in the Caribbean Antilles, specifically the Central Cordillera region of the Dominican Republic, during the Terminal Classic Drought (~1200–850 cal yr BP) using $\delta^2H_{n\text{-alkanes}}$ isotope analyses from a sediment core collected at Laguna Castilla. The Laguna Castilla record spans from 2983 cal yr BP to present day based on seven calibrated radiocarbon dates. The $\delta^2H_{n\text{-alkanes}}$ isotope analysis focuses on odd-numbered, long-chain n-alkanes C_{25}, C_{27}, C_{29}, and C_{31}.

For the Laguna Castilla record, similar $\delta^2H_{n\text{-alkanes}}$values are documented for all quantified *n*-alkanes, with a mean of -183‰ up until 1450 cal yr BP and then an increase in $\delta^2H_{n\text{-alkanes}}$ values to a mean of -144‰ until ~700 cal yr BP and then another decrease in $\delta^2H_{n\text{-alkanes}}$ values to -166‰. The highest $\delta^2H_{n\text{-alkanes}}$ values are at ~885 (maximum), 1220, and 750 cal yr BP. The C_{29} n-alkane was chosen as the proxy for paleohydrological activity in this study as it was the most abundant and based on evidence that odd-numbered long-chain terrestrially-sourced alkanes are especially useful in the reconstruction of evaporation to precipitation ratios in the arid and semi-arid tropics (Douglas et al., 2012). The C_{29} alkane data correlate well to the other odd-numbered, long-chain n-alkanes as well as to previously obtained $\delta^{18}O$ data (Lane et al., 2009) indicating that it is an appropriate proxy for the paleohydrological record at Laguna Castilla.

Evidence for increased aridity in the Caribbean region during the Terminal Classic Drought is seen in the Laguna Castilla $\delta^2H_{n\text{-alkane}}$ record through a sharp increase in $\delta^2H_{n\text{-alkane}}$

values starting around 1450 cal yr BP and continuously higher $\delta^2H_{n\text{-alkane}}$ values until a period after ~700 cal yr BP. These $\delta^2H_{n\text{-alkane}}$ values correspond to a decrease in arboreal pollen, an increase in herbaceous pollen, and an increase in $\delta^{18}O$ values, all of which indicate an increase in E/P ratios during this time. The strong correlation of $\delta^2H_{n\text{-alkane}}$ values with $\delta^{18}O$ values (r^2 = 0.79; $p < 0.01$) and relationship with pollen records from Laguna Castilla provide strong evidence that alkane isotopic concentrations are responding to E/P ratios in this region rather than to ecosystem structural changes. The record also shows similar patterns to other studies on aridity during the TCD such as at Laguna Chichancanab (Hodell et al., 2005), Mexico; Laguna Punta Laguna, Mexico (Curtis et al., 1996); Mexican (Kennett et al., 2012) and Belizean (Webster et al., 2007) speleothem records; and low Ti concentrations in sediment of Cariaco Basin (Haug et al., 2003). The increased aridity during this time period suggests that ITCZ dynamics were playing a role in the climate of the Caribbean, with a more southerly mean ITCZ annual position leading to a decrease in precipitation.

Kennedy et al. (2006) used charcoal, pollen, and organic proxies to show evidence of shifting climates and environments in the Cordillera Central region of the Dominican Republic Valle de Bao is located in some of the highest elevations of the Dominican Republic and dominated by highland vegetation with *Pinus*, Cyperaceae, and Poaceae constituting the majority of the pollen present in the Valle de Bao core. Charcoal is present throughout the entire core with the exception of the past 50–100 years at the site. The close relationship between the abundance of pine trees on the landscape and a large amount of charcoal indicates that fire is an important factor in this ecosystem. Furthermore, the fire record at Valle de Bao shows no indication of human settlement or human-ignited fires at the site. A wetter climate around 4000 cal yr BP is inferred from organic sedimentation in the core indicating bog formation at the site. Periods of

aridity are seen at the site between ~3700 and 1200 cal yr BP, inferred from pollen degradation. However, periods of aridity observed in the late Holocene at other study sites in Hispaniola are not as apparent in the Valle de Bao record. Instead, moist conditions are seen during the middle Holocene period, indicated by an increase in moist-forest taxa and the creation of the bog at the site during what is otherwise an arid time in the Caribbean.

Crausbay et al. (2015) provided a climate record of the past ~5900 years based on pollen and charcoal analysis of another sediment core from the Cordillera Central region of the Dominican Republic. Seven pollen zones were delineated. Zone 7 (~5900–5525 cal yr BP) is dominated by tropical montane cloud forest pollen. These pollen types decline in zone 6, after 5525 cal yr BP, with the area becoming more dominated by Poaceae. Zone 5 (4323–1269 cal yr BP) remains a period where the vegetation is comprised mostly of grasses. After 1269 cal yr BP, in zone 4, *Pinus* pollen percentages increase sharply, indicated a shift to a pine savanna. Grasses began to decline at 586 cal yr BP as the region shifted to a closed forest rather than a savanna. Pine remained dominant until 85 cal yr BP, when increases in fern spores occurred, suggesting a wetter climate after this time. From -11 cal yr BP to the present day, the region shifted back towards the tropical montane cloud forest pollen. The distinct changes in vegetation at the site coincided with migration and position of the ITCZ, with the cloud forest taxa most prominent at the site during times of a more northerly ITCZ position, which brought increased convective activity to the area. This study highlights the importance of the ITCZ in the climate of Hispaniola.

LeBlanc et al. (2017) identified major hurricane events and explored how these events related to shifts in vegetation and fire in a sediment core from a coastal lagoon named Laguna Alejandro, a hypersaline lake located in the southwestern Dominican Republic, with vegetation

mainly consisting of xeric to sub-xeric coastal scrub, with deciduous broadleaf dry forest taxa in the wider region. There have been at least 21 historically documented hurricanes in the region since 1851, with exceptionally strong hurricanes causing overwash onto the barrier and into Laguna Alejandro.

Two unique zones were identified in the Laguna Alejandro sediment core, with zone 1 recorded as ~330-present cal yr BP (43–0 cm) and zone 2 from ~960–330 cal yr BP (160.5–43 cm). Eight hurricane events were recorded throughout the core, with the highest number of closely spaced events taking place in zone 1. The oldest hurricane event (~930 cal yr BP), was identified by gastropod shells overlain with mangrove peat and negative $\delta^{18}O$ values due to hurricane induced meteoric waters. Hurricane events at ~800 and ~730 cal yr BP were also denoted by negative $\delta^{18}O$ values as well as an increase in plant macrofossils, most likely leaf fragments. Hurricane events at ~530 and ~500 cal yr BP were only observed through negative $\delta^{18}O$ values. In zone 1, hurricane events at ~330, ~260, ~210, ~200, and ~170 cal yr BP were identified through an increase in clastic layers of sediment and coarse sand particles, but poor ostracod preservation prevented accurate $\delta^{18}O$ corroboration. The highest pollen concentrations were found in zone 2, which consisted of mainly lowland dry forest taxa, while zone 1 consisted of scrub and sedges. Charcoal concentrations were highest from ~920–780 cal yr BP, with the highest being after the ~910 hurricane event at ~850 cal yr BP.

Laguna Alejandro was most likely a fresh to brackish wetland from ~960–330 cal yr BP when an increase in coarse sand particles from a high energy deposition event created a lacustrine environment. This is seen through mangrove mortality as well as peat collapse in the sediment core. This suggests that mangroves may be especially sensitive to hurricane events and the boundary of clastic sediment and peat at ~330 cal yr BP may indicate a lowering of the lake

level with the frequent hurricanes recorded after ~330 cal yr BP leading to the overall peat collapse. Some hypotheses suggest peat collapse could have resulted from increased tectonic activity, yet the clear sand overwash during this time provides evidence that this shift is from cyclone activity in the area. The increase in clastic sediments in the Laguna Alejandro core from ~200-present cal yr BP agrees with documented historical records of hurricane activity for the region. The earliest hurricane event at ~910 cal yr BP is supported by high gastropod activity, potentially due to increased precipitation, and an increase in macroscopic charcoal at ~850 cal yr BP may be due to increased fuel load and insolation leading to an increase in fire activity. The hurricane may have prevented tropical dry forest recovery as shown by a decrease in the percentage of Fabaceae pollen. These results are consistent with the other studies conducted in the southern United States and Nicaragua. Additionally, levels with extremely negative $\delta^{18}O$ values, but no clastic sediment or increased plant macrofossils, may provide evidence that stable oxygen isotopes from gastropods are a more sensitive proxy to hurricane activity than others. $\delta^{18}O$ values are also consistent with other studies that indicate moister conditions from 1000-700 cal yr BP during the Medieval Warm Period and increased charcoal during this period could be related to climate rather than hurricanes. Additionally, brief freshening periods and a return to drought around ~220 cal yr BP, and the high hurricane overwash from ~330 cal yr BP to present, support studies on high precipitation variability in the circum-Caribbean region during the Little Ice Age (LIA). Overall, suggestions of more arid conditions around ~540 cal yr BP match records of southerly ITCZ movement associated with the LIA.

C. Dynamics and Drivers of Caribbean Climate

There are multiple large-scale climate dynamics that affect precipitation in the Caribbean region. Gamble and Curtis (2008) established a five-part Caribbean climate

conceptual model consisting of the North Atlantic high pressure cell (NAHP), the Caribbean low-level jet stream (CLLJ), subsidence caused by Central America convection, basin-wide increased wind shear, and divergence around Jamaica. Furthermore, these Caribbean climate dynamics are strongly associated with the El Niño Southern Oscillation (ENSO) and NAO, creating a spatially and seasonally diverse climate pattern (Giannini et al., 2000; 2001a; 2001b). Specifically, ENSO cycles tend to influence precipitation patterns more in the western Caribbean and NAO cycles influence precipitation more in the southeastern Caribbean (Jury et al., 2007). This diversity makes the climate drivers of the Caribbean a complex topic of research.

Typically, precipitation in the Caribbean acts on a bimodal structure with year-round precipitation reaching peaks from May–June and September–October accompanied by a seasonal dry period in the summer, commonly referred to as the mid-summer drought (MSD) (Magaña et al., 1999; Curtis, 2002; Gamble et al., 2008; Gamble and Curtis, 2008). The bimodal precipitation regime tends to be stronger in the western Caribbean than in the eastern Caribbean (Giannini et al., 2000). Additionally, the MSD occurs typically from May–June in the eastern Caribbean and from June–July in northwestern Caribbean (Curtis and Gamble, 2008; Gamble and Curtis, 2008).

The spatial and seasonal variations of the MSD in the Caribbean have led to multiple hypotheses on its cause. One hypothesis states the MSD is the result of an intensification of the NAHP into the region during the summer months, creating stronger trade winds that contribute to lower sea-surface temperature (SST) in the North Atlantic by the dispersal of latent heat, ultimately leading to increased subsidence and lower precipitation (Hastenrath,1976; 1978; 1984; Granger, 1985; Giannini et al., 2000; Mapes, 2005; Gamble

and Curtis, 2008). The NAHP moves into the region in July (Hastenrath, 1967; 1976; 1978; 1984; Mapes et al., 2005) and affects the northern Caribbean more so than the rest of the region (Gamble and Curtis, 2008). The movement of the NAHP into the Caribbean causes an intensification of the CLLJ, which is also known as intensified trade winds (Gamble and Curtis, 2008; Cook and Vizy, 2010; Fritz et al., 2011). The strength and location of the CLLJ are factors of the intensity of ENSO and NAO cycles (Whyte et al., 2008). A strong CLLJ disperses heat and moisture from the Caribbean and carries it towards the southern United States (Wang, 2007). These cycles also contribute to SST anomalies (SSTA) of the Pacific and North Atlantic Oceans, which cause climate variability in the region (Giannini et al., 2000). Enfield and Alfaro (1999) found that SSTA of both the Atlantic and Pacific affected the precipitation regimes of the Caribbean. More specifically, an anomalously cool Pacific Ocean and warm Atlantic Ocean, a warm phase of the Atlantic Multidecadal Oscillation (AMO), is associated with more rainfall during the MSD (Sutton and Hodson, 2005; Ting et al., 2009). A cool phase of the AMO and warm Pacific Ocean is associated with dry weather in the region (Enfield and Alfaro, 1999). Spence et al. (2004) found this pattern to be true only for the late wet season in the Caribbean as it is more influenced by ENSO variability. The early wet season in the Caribbean is predominantly influenced by tropical North Atlantic SSTA (Spence et al., 2004).

In recent studies, NAHP, NAO, and the ENSO cycles have been linked to one interseasonal climate signal in the tropics, the Madden-Julien Oscillation (MJO) (Martin and Schumacher, 2011; Curtis and Gamble, 2016). Martin and Schumacher (2011) found that the MJO, a factor in regional SSTAs, convection, and wind circulation, was strongly correlated with precipitation in the Caribbean and rainfall variability. On a strong MJO cycle, precipitation

rates decreased by 50% and was associated with a stronger CLLJ (Martin and Schumacher, 2011). The MJO can be linked to the development of the NAO and ENSO cycles, making it an overarching driver for precipitation in the Caribbean (Curtis and Gamble, 2016).

Angeles et al. (2010) found that the MSD is mostly correlated with vertical wind shear and aerosol particulate dust accumulation from northern Africa. A decrease in vertical wind shear during the month of July correlated highly with a decrease in precipitation across the Caribbean and a 90% increase in vertical wind shear led to a 67% increase in precipitation. Angeles et al. (2010) proposed that the combined influence of a decrease in vertical wind shear in July and an increase in aerosol particulates during the summer months could be the cause of the bimodal pattern of rainfall in the region.

The climate drivers of the Caribbean region are numerous. During the wet season in the Caribbean, high rainfall is associated with weak northeast trade winds, warm Atlantic SST, and cool Pacific SST (Enfield and Alfaro, 1999). Weaker trade winds typically produce greater tropospheric instability, leading to an increase in precipitation (Enfield and Alfaro, 1999). While these associations can explain general causes of precipitation, the two wet seasons in the Caribbean appear to stem from differing sources (Gamble and Curtis, 2008). The early wet season (May–June) is associated with North Atlantic SSTA, while the latter season (September–October) is associated with SSTA in the equatorial Pacific and Atlantic (Chen and Taylor, 2002; Taylor et al., 2002). These examples illustrate some of the complexities of the ocean-atmosphere dynamics affecting the Caribbean. In light of on-going anthropogenic climate change, it is especially crucial to understand the climate drivers of the region. The Caribbean is expected to see increased temperature around 2 ℃ and more extreme precipitation patterns (Singh, 1997). The region overall is expected to see changes in precipitation varying from -39% to +11% and

there is strong consensus that the Greater Antilles region will experience the most precipitation decreases (IPCC, 2007).

D. ITCZ Movement in the Caribbean

An important climate dynamic throughout the Holocene in the Caribbean region is a tendency toward increased aridity and periods of drought associated with periods in which the ITCZ does not migrate as far northward during the northern hemisphere summer (Schneider et al., 2014) Multiple studies have found increasing evidence for two periods of drought in the Caribbean during time periods commonly referred to as the Terminal Classic Drought (approximately 1200–900 cal yr BP) and the Little Ice Age (approximately 650–100 cal yr BP) (Linsley et al., 1994; Haug et al., 2001; 2003; Nyberg et al., 2001; Lachinet et al., 2004; Hodell et al., 2005; Beets et al., 2006; Peterson and Haug, 2006; Donnelly and Woodruff, 2007; Mangini et al., 2007; Lane et al., 2009; 2011; 2014; Bhattacharya et al., 2017). Records from the marine sediment of the Cariaco Basin off the north coast of Venezuela have shown a climatic shift towards drier conditions in the Central America region starting roughly 5400 years ago (Haug et al., 2001). Titanium and iron abundances in these samples are dependent on rainfall, as more (less) rainfall provides more (less) sediment runoff to the basin, causing increased (decreased) heavy metal levels in the sediment. Therefore, the more southerly position of the ITCZ is reflected by lower concentrations of titanium and iron in the Cariaco samples, reflecting decreased rainfall in Venezuela (Haug et al., 2001; 2003).

The shift in mean position of the ITCZ, due to a decrease in solar insolation during the LIA, resulted in temperature reductions in both the Atlantic and Pacific (Lane et al., 2011). These temperature decreases could have been as great as 2–3 ℃ in the North Atlantic (Nyberg et al., 2002; Winter et al., 2000). The decrease in SSTs across the Northern Hemisphere caused

changes in the cross-equatorial gradient of sea surface temperatures, preventing the ITCZ from migrating as far north toward the Northern Hemisphere as it regularly does (Lane et al., 2011). Changes in the cross-equatorial gradient led to an intensification of the CLLJ in the Northern Hemisphere during the LIA and the Terminal Classic Drought, which acted to disperse latent heat and moisture from sea surfaces, furthering a decrease in SSTs (Wang, 2007; Fritz et al., 2011). Further evidence for a southerly ITCZ throughout the LIA is provided by increased precipitation in the Southern Hemisphere while the Northern Hemisphere was experiencing increased aridity (Haug et al., 2001; Baker et al., 2001).

During the TCD, evidence from oxygen isotope, hydrogen isotope, magnetic susceptibility, and sediment composition has corroborated that there was increased aridity that could have been caused by a southerly shift in the ITCZ (Haug et al., 2003; Lane et al., 2009; 2014; Nyberg et al., 2001; Beets et al., 2006; Donnelly and Woodruff, 2007). However, multiple atmospheric and oceanic drivers could have caused the ITCZ shifts of the LIA and the TCD. Some researchers have linked periods of aridity to an increase in the NAHP and the Atlantic Meridional Overturning Circulation (AMOC) (Bhattacharya et al., 2017). Periods of drought in southern Central America and northern Mexico are related to AMOC strength and intensification of NAHP (Bhattacharya et al., 2017). Others have suggested that strong El Niño events led to the decrease in SST gradients and increased trade winds, ultimately leading to the southerly shift of the ITCZ (Fedorov and Philander, 2000; Haug et al., 2001; Nyberg et al., 2002). Overall, the ITCZ could have shifted southward by as much as 500 km during the Little Ice Age (Sachs et al., 2009), associated with intense aridity in the Caribbean region.

Some researchers have proposed that not all of the Caribbean experienced intense aridity associated with shifts in the migrational pattern of the ITCZ. Burn et al. (2016)

interpreted oxygen isotope data from a sediment core in Barbuda to indicate variability in rainfall during the Little Ice Age rather than increased aridity. The evidence of variable LIA rainfall on Barbuda matches some evidence from Jamaica, Cuba, and Belize (Kennett et al., 2012; Fensterer et al., 2013; Burn and Palmer, 2014; Burn et al., 2016), but Lane et al. (2011) found dry LIA conditions on Hispaniola. These differences illustrate the complexity of past climate in the Caribbean and the need for additional records.

E. Previous Proxy Analyses at Laguna Saladilla

Laguna Saladilla was cored in 2001 by Sally Horn and Ken Orvis using a Colinvaux-Vohnout locking piston corer (Colinvaux et al., 1999) operated on a floating raft near the north shore of the lake (Caffrey et al., 2015). Once the sediment core was transported to the University of Tennessee, it was cut in half and material was sub-sampled for accelerator mass spectrometry (AMS) radiocarbon dating. Twenty-six radiocarbon dates were obtained on wood, charcoal, plant remains and bulk sediment (Table 1). Caffrey took samples at 10–12 cm intervals through the sediment core for pollen and loss-on-ignition analysis (Dean, 1974; Caffrey et al., 2015). Pollen preparation followed the standard procedure outlined by Faegri and Iverson (1989). Additionally, microscopic charcoal was analyzed following a modified version of the point-counting procedure of Clark (1982). Microscopic manganese fragments were also quantified in this manner. Diatoms were analyzed in 10-cm intervals along the sediment core following a procedure by Renberg (1990). Finally, shells in the sediment core were identified based on Abbott (1954) and Abbott and Morris (1995). The Saladilla record comprises three

Table 1: Radiocarbon Dates for Laguna Saladilla

Sample	Depth (cm)	Material Dated	Uncalibrated (^{14}C yr BP)	Calibrated Age Year B.P (2-sigma)	Relative Area Under Probability Curve	Median Probability (cal yr BP)
AA82654	73	Bulk Sediment	175 ± 32	34 – 1	0.178	180
				116 – 72	0.077	
				227 – 134	0.547	
				296 – 252	0.197	
AA82659	88	Wood	184 ± 32	33 – 1	0.174	180
				78 – 74	0.004	
				99 – 81	0.023	
				114 – 106	0.009	
				224 – 136	0.566	
				300 – 254	0.221	
Beta-174192	127	Plant Material	280 ± 40	1 – 2	0.002	371
				169 – 153	0.043	
				343 – 282	0.359	
				465 – 346	0.594	
AA82664	161	Bulk Sediment	907 ± 33	754 – 744	0.030	838
				915 – 756	0.969	
Beta-228998	199	Wood	1230 ± 40	1267 – 1063	1.000	1163
Beta-160457	251	Wood	1770 ± 60	1825 – 1552	0.997	1689
				1857 – 1853	0.003	
Beta-160458	273	Wood	2320 ± 40	2167 – 2163	0.002	2340
				2242 – 2179	0.144	
				2459 – 2302	0.852	
AA82655	284	Wood	2375 ± 36	2492 – 2336	0.943	2407
				2607 – 2602	0.005	
				2678 – 2642	0.050	

Table 1 (continued): Radiocarbon Dates for Laguna Saladilla

Sample	Depth (cm)	Material Dated	Uncalibrated (^{14}C yr BP)	Calibrated Age Year B.P. (2-sigma)	Relative Area Under Probability Curve	Median Probability (cal yr BP)
AA82652	326	Wood	2401 ± 34	2498 – 2346	0.862	2428
				2613 – 2595	0.027	
				2690 – 2636	0.109	
AA82656	331	Wood	2404 ± 34	2500 – 2347	0.846	2431
				2614 – 2594	0.032	
				2693 – 2636	0.120	
Beta-176225	370	Wood and Bark	3800 ± 40	4031 – 4008	0.018	4189
				4299 – 4081	0.935	
				4354 – 4327	0.026	
				4387 – 4369	0.013	
				4400 – 4392	0.005	
AA82666	373	Bulk Sediment	2591 ± 40	2591 – 2504	0.139	2736
				2634 – 2615	0.044	
				2780 – 2696	0.815	
AA82661	411	Wood	2443 ± 34	2543 – 2358	0.608	2500
				2575 – 2560	0.023	
				2618 – 2559	0.141	
				2702 – 2630	0.250	
AA82667	495	Charcoal	2527 ± 41	2748 – 2486	1.000	2602
AA82653	557	Bulk Sediment	2758 ± 34	2929 – 2777	0.983	2849
				2943 – 2934	0.016	
AA82657	592	Wood	3080 ± 35	3185 – 3190	0.007	3291
				3376 – 3209	0.993	
Beta-176226	625	Plant Material	2690 ± 40	2860 – 2748	1.000	2797

Table 1 (continued): Radiocarbon Dates for Laguna Saladilla

Sample	Depth (cm)	Material Dated	Uncalibrated (14C yr BP)	Calibrated Age Year B.P. (2-sigma)	Relative Area Under Probability Curve	Median Probability (cal yr BP)
AA82663	654	Bulk Sediment	3231 ± 42	3360 – 3379	1.000	3453
AA82668	692	Plant Material	3364 ± 42	3538 – 3480	0.132	3606
				3533 – 3493	0.071	
				3694 – 3552	0.925	
AA82660	712	Wood	3364 ± 35	3487 – 3484	0.003	3607
				3691 – 3553	0.882	
β160459	715	Wood	3420 ±40	3732 – 3574	0.847	3672
				3774 – 3744	0.055	
				3826 – 3789	0.097	
AA82662	717	Bulk Sediment	3687 ± 36	4159 – 3854	0.973	4029
				4177 – 4171	0.003	
AA82665	730	Bulk Sediment	3687 ± 61	4032 – 4226	0.022	4027
				4416 – 4081	0.978	
AA82651	792	Wood	6623 ± 46	7574 – 7437	1.000	7513
AA82658	819	Wood	6760 ± 41	7675 – 7569	1.000	7617
Beta-160460	845	Wood	7210 ± 40	8071 – 7955	0.802	8016
				8158 – 8085	0.197	

[1.] Lab codes are as follows: AA: The Arizona AMS Laboratory. Beta: Beta Analytic, Inc. Sample codes, depth, material dated, and ^{14}C ages are from Caffrey et al. (2015).

[2.] Calibrated age ranges, relative areas, and median probabilities are updated from Caffrey et al. (2015. They were calibrated using CALIB 7.0.2 (Stuvier and Reimer, 1993) and the InCAL13 database (Reimer et al. 2013).

zones of marine, brackish and freshwater conditions. Zone 3 (8030–5550 cal yr BP) contains abundant marine mollusk shells. This zone of the sediment core has poor pollen preservation. Three levels with countable pollen contained high percentages of *Rhizophora* (red mangrove) pollen, along with pollen of other arboreal taxa and herbs. Zone 2 (5550–2500 cal yr BP) contains predominantly non-arboreal pollen, such as Poaceae, Asteraceae, Cyperaceae, and *Typha*. Zone 2 is separated into two subzones, zone 2b (5550–2500 cal yr BP) and zone 2a (3500–2500 cal yr BP). Charcoal abundance begins to rise in zone 2a. Mollusk shells are much less common in zone 2, and the taxa are markedly different. Zone 2a contains mostly open-water species at the bottom of the section, moving into tidal and very shallow subtidal species near the top of zone 2a. Zone 1 (2500 cal yr BP to present) contains the highest non-arboreal pollen counts, mostly from Amaranthaceae and Poaceae. Arboreal taxa such as *Pinus* and *Rhizophora* decline sharply after 2500 cal yr BP. Zone 1 only contains one contemporaneous mollusk shell, from a species associated with brackish water, near the base of the zone. Diatom samples show a similar pattern, as there is a shift from marine and brackish taxa between zone 3–2a to freshwater/brackish taxa from zone 1b–1a (Caffrey et al., 2015).

The pollen, charcoal, mollusk shell, and diatom assemblages show a transition at Laguna Saladilla from marine to brackish to freshwater influences. The marine phase was from 8030–5550 cal yr BP and is indicative of rising sea level or increased open-water estuaries. Slow sedimentation in zone 1 also provides evidence of deeper open-water at the site. The open-water mollusk taxa that dominate the marine phase of Laguna Saladilla begin to disappear in zone 2. From 5550–2500 cal yr BP, the shift to shallow-living mollusk taxa indicates that Laguna Saladilla became a more freshwater environment. More evidence of a freshwater environment is indicated by a rise in *Typha* and Cyperaceae pollen. Sedimentation

increased greatly at 3680 cal yr BP, which could be a sign of the lake becoming a closed basin. The freshening of Laguna Saladilla could be a sign of increased precipitation in the region, increased stream flow, lower sea level, or geomorphic changes. However, an increase in microscopic charcoal and *Pinus* pollen provides evidence of overall drier conditions at the site during this time. From 2500 cal yr BP to the present, Laguna Saladilla was in a freshwater phase, as indicated by a shift away from mollusk assemblages characterized by brackish conditions and the decline or disappearance of marine or brackish diatoms. The pollen record for zone 1 provides evidence of dry conditions, with an abundance of weedy pollen types such as Amaranthaceae and low arboreal taxa. The driest period occurred ~1570 cal yr BP, illustrated by especially high Amaranthaceae and decreased *Typha*.

The previous research conducted by Caffrey et al. (2015) shows that important climatological changes have been occurring along the northern coast of Hispaniola for the last 8000 years. However, more proxy work is needed to truly understand the role that climatic drivers and geomorphic factors had on changes in the environment. Shifts to a more arid climate broadly match reconstruction of ITCZ patterns in the Late Holocene at other sites (Haug et al., 2001), but changes in signals of aridity at Laguna Saladilla could also be affected by sea level changes or tectonic uplift. A detailed precipitation record from Laguna Saladilla will be useful to understand how environmental changes at the site were influenced by climatic drivers such as the ITCZ, relative sea level changes, fluvial dynamics, or other factors.

CHAPTER III

STABLE ISOTOPE ANALYSIS OF CLIMATE AT LAGUNA SALADILLA

A. Methods

i. Age Model

A new age model for the Laguna Saladilla core was developed using the R software version 3.4.3 Bacon package based on radiocarbon dates from Caffrey et al. (2015) (R Core Team, 2017; Blaauw and Christen, 2018).

ii. Sampling

The Laguna Saladilla was sampled for sediment core for $\delta^2H_{n\text{-alkanes}}$ analysis at 39 levels to match the positions of samples previously taken for pollen and charcoal analyses by Caffrey et al. (2015). All samples were taken from the upper 230 cm of sediment, ranging from 2000– -40 cal yr BP. Sample intervals were 3–4 cm wide to obtain a wet mass of at least 40 g. Subsamples in 1 cm^3 width were taken from the center location of each $\delta^2H_{n\text{-alkanes}}$ sample for δ^2H_{Bulk}, $\delta^{13}C$, and $\delta^{15}N$ analysis.

iii. Compound-Specific Hydrogen Isotopes

The 39 $\delta^2H_{n\text{-alkanes}}$ samples were oven-dried at 60°C for 72 hours removed and then ground with a mortar and pestle to a coarse powder consistency. 50 mL of a 2:1 dichloromethylene to methanol (DCM) solvent was added to each sample and then shaken using a soniccator and centrifuged at ~1500 RPM for fifteen minutes. The liquid solvent was extracted and further filtered through a glass fiber filter to ensure the removal of any loose particles. The remaining material was evaporated to ~5mL using a rotary evaporator. This process was repeated a total of three times and the remaining lipids were dried under a stream of nitrogen (N_2) gas.

The leftover bulk sediment was discarded in compliance with USDA protocols for foreign sediment.

The lipids extracted from the sediment then were subjected to a process of saponification to separate the neutral lipids from the non-neutrals by adding 3 mL of 5% potassium hydroxide (KOH) in a 80:20 MeOH:H_2O solution to each sample. The samples were then sealed with N_2 gas and heated in an oven at 80 °C for 1 hour after ensuring that each sample had a basic pH level between 12 and 14. The saponified neutral lipids were separated from the non-saponified fraction using 3 mL of hexane solvent and centrifuging at approximately 1500 RPM for five minutes, and then dried under a stream of N_2 gas. The non-saponified fraction was archived for future use.

Next, the samples were separated further based on lipid class. The neutral lipids were dissolved in 8 mL of DCM and pulled through a glass column loaded with silica gel rinsed thoroughly with DCM to avoid contamination. After the silica gel-loaded glass column was thoroughly rinsed through with DCM, MeOH was added and pulled through the column to separate out the MeOH fraction of the lipids. The MeOH fraction was archived for later analysis. All samples were dried under a stream of N_2 gas.

Finally, the Laguna Saladilla samples were prepared using urea adduction. 1.5 mL of a 2:1 hexane to acetone mixture were added to each sample and then a solution of 1 g of urea to 4 mL of methanol was warmed on a hot plate at 50 °C and added dropwise to each sample while being shaken on a vortex. The samples were placed in a freezer overnight and then dried under a stream of N_2 gas. Next, 3 mL of DCM were added to each sample and centrifuged down at 1500 rpm for 15 minutes. The top part of the sample was removed with a pipette as the non-adducts and saved for later analysis. This process was repeated three times. The adducts were recovered

by dissolving the remaining material in 10 mL of DCM extracted water and extracted with 2 mL of hexane. This process was repeated twice to ensure all the adducts were recovered. The recovered adducts were blown dry under a stream of N_2 gas and then extracted with 200 µL of hexane to be loaded into vials for analysis. Additionally, 100 µL of a known alkane squalane standard was added to each sample.

Samples were analyzed at the University of North Carolina-Wilmington Isotope Ratio Mass Spectrometry Laboratory on a Thermo Delta V plus mass spectrometer interfaced with a Thermo 1310 gas chromatograph via an Isolink II device, with the assistance of Dr. Chad Lane. All samples were analyzed in duplicate. IU B4 alkane standards (provided by A. Schimmelmann) with known hydrogen isotope composition were run after every fourth sample to reduce uncertainty and measure instrument precision. Hydrogen isotopic compositions are reported in the standard δ-per mil notation relative to VSMOW where R = $^2H/^1H$ and

$$\delta D = 1000[(R_{sample}/R_{standard})-1]$$

Alkane peaks and their corresponding $\delta^2H_{n\text{-alkanes}}$ value in odd-number alkane chains C_{23}-C_{33} were identified and calculated using Isodat software. Results were corrected based off calculations by Polissar and D'Andrea (2014) using the raw data and IU B4 alkane standard runs.

iv. Bulk Stable Isotopes

Samples of 1 cm^3 volume were taken from all 39 sampled levels of the Laguna Saladilla sediment core for δ^2H_{Bulk} analysis in hopes of extending the record from levels where *n*-alkane abundance was too low to provide accurate interpretation. The samples were split into two portions, one to be acidified and one to remain non-acidified. The acidification process followed a protocol of fumigating samples moistened with distilled water with 12 N hydrochloric acid

(HCl) for two hours in a desiccator and then venting them over 48 hours. The samples were then dried on a hot plate at ~50 °C until all water and acid evaporated. A target weight for the dried 39 δ^2H_{Bulk} samples based on previous loss on ignition analysis was met and the samples were loaded into silver capsules. Sample preparation took place at the University of Tennessee's Laboratory of Paleoenvironmental Research and then were analyzed at the University of North Carolina-Wilmington Isotope Ratio Mass Spectrometry Laboratory on a Thermo Flash HT Plus elemental analyzer interfaced with Thermo Delta V Plus stable isotope mass spectrometer, with the assistance of Dr. Chad Lane. All samples were run in 100% duplicate. Hydrogen samples were run with repeated analyses of USGS 71 and USGS 62 glutamic acid standards to ensure instrument precision was at ±1.8‰. Hydrogen isotopic compositions are reported in standard δ-per mil notation, with values relative to VSMOW-SLAP scale where R = 2H/1H and:

$$\delta^2H_{Bulk} \text{ (permil)} = 1000[(Rsample/Rstandard)-1]$$

Fifteen 1 cm^3 samples of the acidified fraction were additionally analyzed for stable $\delta^{13}C$ and stable $\delta^{15}N$ isotope analysis to better understand terrestrial and aquatic inputs to the lake. The stratigraphic levels for $\delta^{13}C$ and $\delta^{15}N$ isotope sampling were selected to match previous levels sampled for loss on ignition analysis conducted by Caffrey et al. (2015). Isotope samples were run with USGS 40 and USGS 41 glutamic acid standards which indicated instrument precision was at ±0.33‰. $\delta^{13}C$ and $\delta^{15}N$ isotopic compositions are reported in standard δ-per mil notation, with $\delta^{13}C$ values relative to the Vienna-Pee Dee belemnite (V-PDB) marine carbonate standard, $\delta^{15}N$ values relative to AIR, where R = 13C/12C or 15N/14N and:

$$\delta^{13}C \text{ or } \delta^{15}N \text{ (permil)} = 1000[(Rsample/Rstandard)-1]$$

v. Comparison of Hydrogen Isotopes

δ^2H_{Bulk} acidified and non-acidified isotopes were compared to each other and to $\delta^2H_{n\text{-alkanes}}$ isotopes using R version 3.4.3 for statistical computing. Correlation tests were run on a variety of combinations, including comparisons of acidified to non-acidified δ^2H_{Bulk} isotopes and each set of δ^2H_{Bulk} isotopes to each of the 6 (C_{25}-C_{33}) long-chain odd-numbered *n*-alkanes. Tests were based on the $\alpha = 0.05$ significance level. I plotted the results alongside previous pollen and charcoal proxies with the C2 program (Juggins, 2007). Proxies were plotted by age rather than depth, based on interpolated ages created by the Bacon age model for Laguna Saladilla.

B. Results

i. Bacon Age Model

The new age model for the Laguna Saladilla (Figure 2) updates the model in Caffrey et al. (2015), using Bacon software based on Bayesian statistics.

ii. Paleoenvironmental Reconstruction

Compound-Specific Hydrogen Isotopes

Of the 39 samples taken for $\delta^2H_{n\text{-alkanes}}$ isotope analysis, only 21 samples contained adequate abundances of odd-numbered long-chain *n*-alkanes for paleoenvironmental reconstruction (Figure A.1). These 21 samples all came from the lower part of the section of the Laguna Saladilla core I sampled, from 142 cm to 244 cm. The age of the $\delta^2H_{n\text{-alkanes}}$ record spans from 545–1701 cal yr BP, based on the new BACON age model. For odd-numbered long-chain *n*-alkanes C_{25}-C_{33}, the highest (least negative) $\delta^2H_{n\text{-alkanes}}$‰ V-SMOW values were all found at 209 cm depth, corresponding to an age of 1249 cal yr BP or 701 CE. As these odd-numbered,

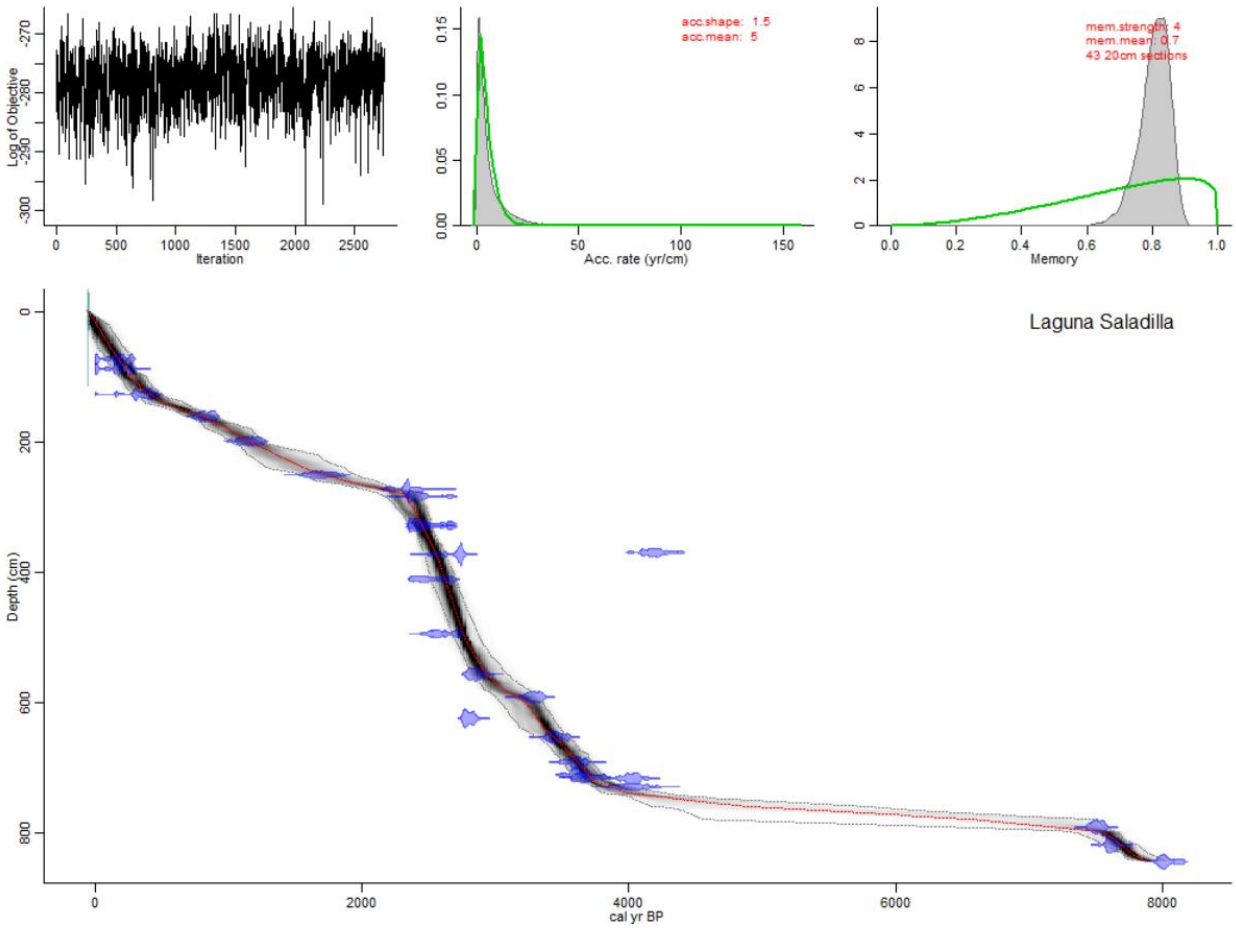


Figure 2: Laguna Saladilla age-depth model. Created using the 'rbacon' package (v.2.3.4; Blaauw and Christen, 2018) in the R statistical environment (v.3.4.3; R Core Team 2017) and the IntCal13 radiocarbon calibration curve (Reimer et al. 2013), based on radiocarbon dates reported by Caffrey et al. (2015).

long-chain *n*-alkanes are dominantly controlled by the amount effect and E/P ratios at the site, the results indicate that the driest period at Laguna Saladilla occurred at this time, slightly before or at the start of the Terminal Classic Drought. The lowest (most negative) $\delta^2H_{n\text{-alkanes}}$ ‰ V-SMOW values for all measured *n*-alkanes were at the bottom of the sampled section with minima at depths of 223 cm for C_{33}, 229 cm for C_{25}, 239 cm for C_{23}, C_{27}, and C_{31}, and 249 cm for C_{29}. These results indicate that the wettest period in the record at Laguna Saladilla occurred from 1454–1701 cal yr BP or 496 CE to 249 CE. Overall, the Laguna Saladilla $\delta^2H_{n\text{-alkanes}}$ isotope record does not show extreme variations in $\delta^2H_{n\text{-alkanes}}$ values, with an average variation of 30‰, which could suggest a history of relatively stable precipitation and E/P ratios at the site.

Bulk Hydrogen Isotopes

Analysis of the hydrogen isotope composition of bulk organic matter was run on both acidified and non-acidified samples. The δ^2H_{Bulk} isotope values for the acidified and non-acidified samples were positively correlated with a Pearson's r value of 0.74 (p-value <0.01) (Table 2). The comparison suggests that the acidification process did not cause a significant difference in δ^2H_{Bulk}values.

The maxima of the δ^2H_{Bulk} values occur in both the acidified and non-acidified samples in the uppermost part of the core, with the non-acidified maximum (not shown) of -67.6‰ at 15 cm depth and the acidified maximum of -74.5‰ δ^2H_{Bulk} value at 69 cm depth, corresponding to -4 cal yr BP and 163 cal yr BP, respectively. The minima of δ^2H_{Bulk} values occur in the lower part of the core, with a minimum of -95.8‰ δ^2H_{Bulk} at 194 cm for the non-acidified samples (not shown) and -104.5‰ δ^2H_{Bulk} at 209 cm for the acidified samples, corresponding to 1107 cal yr BP and 1249 cal yr BP, respectively. Overall, the δ^2H_{Bulk} isotope record shows higher δ^2H_{Bulk} values in the upper-half of the sediment core above 159 cm depth, with an average of -78.0‰ for

the non-acidified samples and -85.2‰ for the acidified samples compared to an average of -87.2‰ for the non-acidified samples and -94.9‰ for the acidified samples in the lower section of the sediment core.

Bulk Carbon and Nitrogen Isotopes

For the $\delta^{13}C$ and $\delta^{15}N$ isotopes, the highest $\delta^{13}C$ value of -17.2‰ occurs at 179 cm depth while the lowest value of -27.2‰ occurs at 39 cm depth. The lowest $\delta^{13}C$ values occur at the uppermost and lowermost sections of the Laguna Saladilla sediment core with the highest values contained in the middle section, suggesting that the driest period in the record is from 179–209 cm depth or 1249–988 cal yr BP (701–962 CE). The $\delta^{15}N$ record does not show the same pattern as the $\delta^{13}C$, with higher values towards the bottom of the core, with the exception of the highest $\delta^{15}N$ value of 4.0‰ at 5 cm depth, and lower values towards the top of the core with a minimum $\delta^{15}N$ value of -0.1‰ at 127 cm depth. The C/N isotope ratio throughout the sampled sediment core ranges from 9.7 to 15.5, suggesting that the Laguna Saladilla contains a mixture of terrestrial and aquatic inputs (Meybeck, 1982; Sharpe, 2007). However, a higher C/N ratio in the uppermost and lowermost section of the core could indicate higher terrestrial input during these times.

iii. Correlation of the Bulk and Compound-Specific Hydrogen Isotopes

The δ^2H_{Bulk} isotope values do not show the expected, positive correlation with the $\delta^2H_{n\text{-alkanes}}$ isotope values. Correlation tests were performed between both the acidified and non-acidified δ^2H_{Bulk} samples and all six odd-numbered, long-chain *n*-alkanes. Of twelve correlation tests performed (Table 2), only three tests showed significant correlations, all three showing a negative correlation between the δ^2H_{Bulk} and $\delta^2H_{n\text{-alkanes}}$ isotope values. The lack of correlation

Table 2: Statistical Results of Correlation Between Hydrogen Isotope Results[1]

	Acidified δ^2H_{Bulk}	Non-Acidified δ^2H_{Bulk}	δ^2H_{C23}	δ^2H_{C25}	δ^2H_{C27}	δ^2H_{C29}	δ^2H_{C31}	δ^2H_{C33}
Acidified δ^2H_{Bulk}		**p<0.01** r=0.74	**p=0.04** r=-0.44	p=0.53 r=-0.14	p=0.07 r=-0.41	p=0.14 r=-0.33	**p=0.01** r=-0.53	p=0.16 r=-0.33
Non-acidified δ^2H_{Bulk}	**p<0.01** r=0.74		p=0.37 r=-0.20	p=0.25 r=-0.26	p=0.45 r=-0.17	**p=0.04** r=-0.45	p=0.06 r=-0.42	p=0.37 r=0.21

[1.] Bolded p-values indicate significant results (p-value<0.05).

between the two hydrogen isotope datasets indicate that the δ^2H_{Bulk} record at Laguna Saladilla cannot be used to extend the $\delta^2H_{n\text{-alkanes}}$ isotope record at levels where *n*-alkane abundance was too low for measurement. While the δ^2H_{Bulk} isotope record is not useful for extending the $\delta^2H_{n\text{-alkanes}}$ isotope record, the pattern of change shows similarities to the pollen and charcoal record developed by Caffrey et al. (2015) and to the stable $\delta^{13}C$ and $\delta^{15}N$ isotope records, suggesting it may still provide a useful paleoenvironmental proxy.

C. Discussion

i. Comparison to Previous Proxy Work at Laguna Saladilla

Comparison of the new δ^2H_{Bulk} and $\delta^{13}C$ isotope records and $\delta^2H_{n\text{-alkanes}}$ isotope record to the pollen and microscopic charcoal record constructed by Caffrey et al. (2015) shows that the δ^2H_{Bulk} and $\delta^{13}C$ isotope records show a stronger match. Higher δ^2H_{Bulk} values at Laguna Saladilla correspond with higher percentages of Cyperaceae, *Typha*, and Poaceae pollen and fern spores and to higher microscopic charcoal concentrations. The $\delta^2H_{n\text{-alkanes}}$ isotope record also shows some similarities to the pollen record, specifically to Amaranthaceae pollen, but as the $\delta^2H_{n\text{-alkanes}}$isotope data are not available for the upper part of the core section, a full comparison is impossible.

Fourteen samples from the Caffrey et. al (2015) microscopic charcoal record overlapped with the δ^2H_{Bulk}, $\delta^{13}C$, and $\delta^{15}N$ isotope record from this study. Three instances of higher microscopic charcoal area concentration (mm^2/cm^3) correspond to sections of the sediment core with the highest δ^2H_{Bulk} values at the uppermost and the lowermost sections of the core. While the increased microscopic charcoal concentrations in these levels indicate increased fire activity at Laguna Saladilla and the surrounding region, this does not necessarily imply that conditions were drier overall at these times. The seasonality of precipitation or the availability of lightning

could affect the charcoal record, as increased lightning from convective activity could lead to an increase in fire activity. The microscopic charcoal concentrations show an inverse relationship with the $\delta^{13}C$ values, with the uppermost and lowermost section of the Laguna Saladilla core containing the lowest $\delta^{13}C$ values. This finding also indicates that increased charcoal accumulation does not match with increased aridity at Laguna Saladilla. Microscopic charcoal concentrations show no clear relationship with the $\delta^{15}N$ isotope record.

The $\delta^{2}H_{Bulk}$ isotope record generally shows an inverse relationship with Amaranthaceae pollen percentages. However, the $\delta^{13}C$ values have a positive relationship with Amaranthaceae pollen. The relationship between high $\delta^{13}C$ values and high Amaranthaceae pollen percentages is consistent with the interpretation of Caffrey et al. (2015) that the high Amaranthaceae percentages indicates drier conditions beginning ca 2500 cal yr BP at Laguna Saladilla. Higher $\delta^{13}C$ values indicate the presence of more C_4 plants, such as Amaranthaceae, which tend to thrive in a drier climate than C_3 plants (Rajendrudu et al., 1986). Higher $\delta^{13}C$ values can also reflect drought stress in C_3 plants, as an increase in these values correlate with a decrease in mean annual precipitation (Diefendorf et al., 2010; Kohn, 2010).

That the $\delta^{2}H_{Bulk}$ and the $\delta^{13}C$ isotope records show an inverse relationship indicates that the two proxies I investigated do not respond to the same climate controls. It seems that lower $\delta^{2}H_{Bulk}$ values indicate periods of increased aridity, whereas lower long-chain ($\geq C_{25}$) $\delta^{2}H_{n\text{-alkanes}}$ values indicate periods of increased precipitation. I further discuss this apparent discrepancy in the next section.

The $\delta^{2}H_{n\text{-alkanes}}$ isotope record shows little variation when compared to the other proxies studied at Laguna Saladilla. A weak positive relationship is evident between Amaranthaceae pollen percentages and higher long-chain ($\geq C_{25}$) $\delta^{2}H_{n\text{-alkanes}}$ values, as the highest $\delta^{2}H_{n\text{-alkanes}}$

values occur during time dominated by Amaranthaceae and the lowest $\delta^2H_{n\text{-alkanes}}$ values for two chain lengths (C_{27} and C_{31}) occur when Amaranthaceae percentages are at their lowest. But, the $\delta^2H_{n\text{-alkanes}}$ values show an inverse relationship with *Typha* pollen percentages, with the lowermost part of the core containing the highest *Typha* percentages and generally the lowest $\delta^2H_{n\text{-alkanes}}$ values (except for C_{25}) and the highest $\delta^2H_{n\text{-alkanes}}$ values corresponding to a sharp drop-off in *Typha* percentages. These relationships between vegetation and the $\delta^2H_{n\text{-alkanes}}$ isotope record provide evidence of increased aridity during times of higher $\delta^2H_{n\text{-alkanes}}$ values at Laguna Saladilla.

ii. Comparison of Bulk and Compound-Specific Hydrogen Isotopes

The δ^2H_{Bulk} isotope record and the $\delta^2H_{n\text{-alkanes}}$ isotope record at Laguna Saladilla tend to follow an inverse relationship with one another. The lowest (most negative) values for the δ^2H_{Bulk} record occur between 1316–1107 cal yr BP (701–843 CE), whereas the highest (least negative) odd-numbered long-chain ($\geq C_{25}$) $\delta^2H_{n\text{-alkanes}}$values occur within the same time period from 1249 cal yr BP or 701 CE. When compared to other proxies, such as pollen, charcoal, and bulk stable $\delta^{13}C$ isotopes, results indicate that higher $\delta^2H_{n\text{-alkanes}}$values indicate increased aridity at Laguna Saladilla while higher δ^2H_{Bulk} values indicate wetter conditions. The inverse relationship of the δ^2H_{Bulk} record with Amaranthaceae and the $\delta^{13}C$ record support this hypothesis. The δ^2H_{Bulk} record does have a positive relationship with the charcoal record, but due to the extreme aridity of the region, this could suggest that times of lower δ^2H_{Bulk} values and charcoal concentrations contain too little vegetation for increased fire activity.

There could be multiple factors that explain the inverse relationship between δ^2H_{Bulk} and $\delta^2H_{n\text{-alkanes}}$ isotope values at Laguna Saladilla. The hydrogen isotopes in the $\delta^2H_{n\text{-alkanes}}$ record and the δ^2H_{Bulk} record originate from different sources. The isotopic composition for the $\delta^2H_{n\text{-alkanes}}$

record originates from hydrogen isotopes in leaf waxes stored at the time of formation, while the δ^2H_{Bulk} values can originate from a variety of sources, both terrestrial and aquatic. The low C/N ratio throughout the sampled sediment section indicates that much of the organic matter may be sourced from aquatic algae, which could account for the different signal seen in the δ^2H_{Bulk} record and the $\delta^2H_{n\text{-alkanes}}$ record. Additionally, The Rio Masacre could be transporting water and sediment with more negative δ^2H_{Bulk} values from sources high in the Cordillera Central.

The multiple factors in hydrogen isotope source and different fractionations between sources makes interpretation of the δ^2H_{Bulk} record more uncertain than interpretation of the $\delta^2H_{n\text{-alkanes}}$ record. An important factor may be the source of precipitation to the region. Caffrey et al. (2015) stated that the Laguna Saladilla region is heavily influenced by precipitation from polar outbreaks, mainly occurring in the autumn and early winter months (Bolay, 1997). This form of precipitation can result in highly negative δ^2H_{Bulk} values, suggesting that lower values in the δ^2H_{Bulk} record indicate periods of increased precipitation from polar outbreaks, rather than a shift in precipitation amount altogether. A study using the International Atomic Energy Agency's Global Network of Isotopes in Precipitation found that precipitation sourced from polar regions in the winter months (December-February) tends to have lower (more negative) δ^2H values when compared to precipitation occurring during the summer months from convective activity (Araguás-Araguás and Diaz Teijeiro, 2005). More precipitation from polar air outbreaks rather than convective activity at Laguna Saladilla could cause low δ^2H_{Bulk} as seen in the record. This hypothesis would explain why the δ^2H_{Bulk} isotope record tends to show an inverse relationship to the $\delta^2H_{n\text{-alkanes}}$ isotope record and would be consistent with other proxies at the site. Rather than an indicator of precipitation amount at Laguna Saladilla, the δ^2H_{Bulk} values could be more reflective of changes in precipitation source. Time periods when there is precipitation from

mixed sources (polar outbreaks and convective activity) could cause the higher (less negative) δ^2H_{Bulk}values. At Laguna Saladilla, the larger variations in the δ^2H_{Bulk} record compared to the $\delta^2H_{n\text{-alkanes}}$ record and the stronger correlation with other proxies suggest that the δ^2H_{Bulk}isotope proxy is responding to the same climate controls as vegetation and charcoal accumulation, which could reflect changes in precipitation source. Caffrey and Horn (2015) found a relationship between increased charcoal accumulation and increased winter solar insolation at Laguna Saladilla, which they associated with decreased winter precipitation and increased burning. This interpretation would be consistent with the hypothesis that higher δ^2H_{Bulk} values reflect lower precipitation from polar outbreaks. In contrast, the $\delta^2H_{n\text{-alkanes}}$ record appears to be more responsive to precipitation amounts and E/P ratios, as has been documented in other arid to semi-arid tropical environments (Douglas et al., 2012).

However, as the δ^2H_{Bulk} record comprises multiple sources of organic matter and could reflect a variety of possible changes at the site. Higher C/N ratios (13–15) in the uppermost and lowermost sections sampled, indicating higher aquatic inputs into the lake, correspond to higher δ^2H_{Bulk} values. This could indicate that the δ^2H_{Bulk} record responding to changes in organic matter sources from terrestrial plants to aquatic algae, where the terrestrial matter δ^2H_{Bulk} value is fixed at the time of growth and the aquatic matter δ^2H_{Bulk} value is not. This explanation could account for the differences seen between the δ^2H_{Bulk} and $\delta^2H_{n\text{-alkanes}}$ record, as all organic matter in the $\delta^2H_{n\text{-alkanes}}$ record is terrestrially sourced. Similarly, water from the northward flowing Rio Masacre could be transporting more negative δ^2H_{Bulk} values from the Cordillera Central region accounting for the differences in the δ^2H_{Bulk} and $\delta^2H_{n\text{-alkanes}}$ records.

iii. Climate Record and the Terminal Classic Drought at Laguna Saladilla

The δ^2H_{Bulk} record, compared with the $\delta^{13}C$, charcoal, and pollen record suggests that the period from ~1450–250 cal yr BP (~500–1700 CE) was drier than the periods of ~1750–1450 cal yr BP (~200–500 CE) and 250 cal yr BP (1700 CE) to present day. The earliest 300 years of the record (1750–1450 cal yr BP) contain the lowest $\delta^2H_{n\text{-alkanes}}$ values for all odd-numbered, long-chain *n*-alkanes. This period is characterized by higher percentages of *Typha* and Poaceae pollen as well as the highest charcoal concentration, and low $\delta^{13}C$ values. The C/N ratio during this time period suggests a mixture of terrestrial and aquatic inputs into the lake, but the higher C/N ratio (11–13) compared to other times on record could indicate slightly more terrestrial input during this period.

The early wet period ends ~1450 cal yr BP, followed by more arid conditions that persist until ~250 cal yr BP. Within the period of dry conditions is the TCD spanning from approximately ~1250–850 cal yr BP. The highest $\delta^2H_{n\text{-alkanes}}$value ($>C_{25}$) occurs at ~1253 cal yr BP, just at the onset of the TCD. This is also the time of the lowest value in the δ^2H_{Bulk} record. As lower δ^2H_{Bulk} values can signal more precipitation from polar outbreaks in the winter rather than convective activity, this pattern of change would support a more southerly mean position of the ITCZ during the TCD, as this would result in reduced convective precipitation. These findings are consistent with the results of other studies conducted in Hispaniola and the circum-Caribbean (Haug et al., 2003; Lane et al., 2009; 2014; Nyberg et al., 2001; Beets et al., 2006; Donnelly and Woodruff 2007). The dry period at Laguna Saladilla is also characterized by the highest percentages of Amaranthaceae on record, little to no charcoal accumulation, and the highest $\delta^{13}C$ values. The C/N ratio during this period remains in a range that indicates mixed

terrestrial and aquatic inputs to the lake, but lower values compared to the periods of wetter conditions could indicate an increase in aquatic inputs.

The second wet period at Laguna Saladilla begins at approximately 250 cal yr BP and continues up until the present day. This period is characterized by a drop-off in Amaranthaceae pollen percentages, with a sharp increase in ferns and Poaceae. It also contains the highest δ^2H_{Bulk} values on record and the lowest $\delta^{13}C$ values, supporting the idea of a wetter climate with changes in the precipitation source shifting to increased convective activity. Increased convective precipitation shown by the δ^2H_{Bulk} values could also explain the increased fire activity indicated by the peak in charcoal concentration at the top of the record. The highest C/N ratio is seen during this ~300-year period, suggesting the highest input of terrestrial material.

iv. Comparison to Other Study Sites in Hispaniola

Lane et al. (2014) presented evidence of increased aridity in the Caribbean Antilles, specifically the Central Cordillera region of the Dominican Republic, during the Terminal Classic Drought (~1200–850 cal yr BP) using $\delta^2H_{n\text{-alkanes}}$ isotope analyses from a sediment core collected at Laguna Castilla. The Laguna Saladilla records complements the $\delta^2H_{n\text{-alkanes}}$isotope record from this region. Most notably, an increase in aridity represented by the higher $\delta^2H_{n\text{-alkanes}}$ values around 1250–1200 cal yr BP or the onset of the Terminal Classic Drought. The drought-like conditions continue in the region throughout the TCD and this record shows a much more extreme change from wet conditions to dry conditions. The Laguna Saladilla record, on the other hand, shows a much more gradual change in aridity, which could be due to the more stable coastal climate falling in a rain shadow region versus the more variable climate of the Cordillera Central region in the Dominican Republic. However, it does indicate that southerly migration of the ITCZ also causes shifts towards aridity during the TCD at Laguna Saladilla.

Stable oxygen isotope evidence by Lane et al. (2009) for a sediment core from Laguna de Felipe, located near Laguna Castilla, provides more evidence of aridity in the Dominican Republic during the Terminal Classic Drought. The record matches well with the Laguna Saladilla record of increased aridity starting ~1250 cal yr BP, the onset of the "Early Phase" of the TCD. However, the oxygen isotope record from Laguna de Felipe also shows that the Medieval Climate Anomaly had wetter conditions on Hispaniola. This period of wet conditions is not apparent in the Laguna Saladilla proxy record. As Laguna Saladilla is one of the drier regions of the Dominican Republic and falls in the rain shadow region from the Cordillera Septentrional mountain range, it could be that this area did not experience increased rainfall, despite a more northerly ITCZ position.

Crausbay et al. (2015) provided evidence that a shift from tropical montane cloud forest taxa to an ecosystem of pine and grasses correlated with a more southerly placed ITCZ. The shift to a pine savanna ecosystem at the site after ~1269 cal yr BP indicates a more southerly ITCZ position caused drier conditions in the Cordillera Central region of Hispaniola. This finding complements the Laguna Saladilla record, which shows drier conditions beginning at the site ~1250 cal yr BP. Similarly, the increased presence of ferns at the site beginning ~85 cal yr BP suggesting moister conditions at the site follow a similar pattern at Laguna Saladilla with moister conditions starting ~250 cal yr BP up to the present day.

LeBlanc et al. (2017) used sediment overwash and oxygen isotopes to infer hurricane frequency and times of moist/arid conditions at a Laguna Alejandro in the southwestern Dominican Republic. High hurricane frequency found from ~330 cal yr BP up to present day at the site may indicate increased precipitation. These findings match higher δ^2H_{Bulk} values at Laguna Saladilla beginning ~250 cal yr BP, which could also be indicative of increased

precipitation variability at the site. Similarly, inferred arid conditions at the site ~540 cal yr BP match low δ^2H_{Bulk} values seen at Laguna Saladilla. However, moister conditions from 1000–700 cal yr BP at Laguna Alejandro do not coincide with the drier conditions seen at Laguna Saladilla during this period, highlighting the diversity of climate in the Hispaniola region.

v. Climate Dynamics Affecting Precipitation at Laguna Saladilla

The proxy record presented in this study suggest that ITCZ dynamics play a role in precipitation at Laguna Saladilla. Multiple studies have shown that a more southerly positioned ITCZ during the TCD reduced precipitation across the Caribbean (Haug et al., 2003; Lane et al., 2009; 2014; Nyberg et al., 2001; Beets et al., 2006; Donnelly and Woodruff 2007). The more southerly position of the ITCZ has been associated with variability in the strength of the CLLJ and the NAHP, and a decrease in SSTs (Wang, 2007; Lane et al., 2011).

These climate drivers are also linked to large-scale ocean-atmosphere dynamics such as the NAO and AMO (Wang, 2007; Bhattacharya et al., 2017). The strength of the CLLJ is dependent upon the strength of the NAHP. A stronger NAHP causes a stronger CLLJ as it changes sea level pressure and SST. Warmer SST anomalies in the Caribbean, which are related to a positive AMO, are related to lower sea level pressures that cause a weaker CLLJ. During the TCD, cooler SSTs in the Caribbean resulted in a stronger CLLJ. A stronger CLLJ is associated with the transportation of moisture from the Caribbean into the Gulf of Mexico and the United States, causing a decrease of moisture in the Hispaniola region (Wang, 2007). As a strong CLLJ is related to decreased convection and static instability over the Caribbean, cooler sea surface temperatures during the TCD would result in frontal precipitation predominantly sourced from polar outbreaks rather than from convective activity (Wang, 2007). This interpretation is

supported by the δ^2H_{Bulk} record at Laguna Saladilla, as it shows more negative δ^2H_{Bulk} values during the onset of the TCD which could indicate precipitation from a northerly source

The correlation of these climate drivers and dynamics with the ITCZ position and precipitation suggest that they are all important factors driving the hydrology record at Laguna Saladilla. Specifically, the NAHP and CLLJ's relationship with SSTs and sea level pressure are large factors causing differences in precipitation source and amount reaching the coastal area of Hispaniola. The NAHP is typically stronger in the summer months, causing an increase in subsidence and therefore less precipitation reaching the northern Caribbean region (Gamble and Curtis, 2008). Therefore, the NAHP heavily influences the seasonality of rainfall at Laguna Saladilla, leading to more precipitation in the winter months from polar outbreaks rather than from convective activity. As these are influenced by larger ocean-atmosphere dynamics such as the NAO and AMO, precipitation at Laguna Saladilla is likely controlled by a multitude of climate drivers, as elaborated for the region by Bhattacharya et al. (2017).

CHAPTER IV

SUMMARY AND CONCLUSIONS

My thesis research at Laguna Saladilla extends the previous proxy record by Caffrey et al. (2015). The geochemical data from $\delta^2H_{n\text{-alkanes}}$ and δ^2H_{Bulk}, $\delta^{13}C$, and $\delta^{15}N$ isotopes provide evidence of climate change that complement the existing charcoal and pollen record for the site. This study also builds upon the research at sites across Hispaniola and the circum-Caribbean, adding to multiple studies that illustrate the differences and similarities of climate changes throughout the region (Linsley et al., 1994; Haug et al., 2001; 2003; Nyberg et al., 2001; Lachinet et al., 2004; Hodell et al., 2005; Beets et al., 2006; Peterson and Haug, 2006; Donnelly and Woodruff, 2007; Mangini et al., 2007; Lane et al., 2009; 2011; 2014; Bhattacharya et al., 2017). My results provide evidence of the usefulness of δ^2H_{Bulk} isotopes in the reconstruction of paleoenvironments and help document precipitation trends and decipher the climate drivers that may be responsible for precipitation changes at the study site.

The findings of my thesis research reveal that Laguna Saladilla experienced drier conditions during the Terminal Classic Drought, expanding on the findings of other researchers at sites across the Dominican Republic and Hispaniola. However, based on previous research by Lane et al. (2014), precipitation at Laguna Saladilla has not experienced variations as extreme as at other sites in inland Hispaniola. This suggests that the coastal climate and the rain shadow location of Laguna Saladilla yield more stable as well as drier overall conditions compared to other sites.

While the δ^2H_{Bulk} record did not help to extend the $\delta^2H_{n\text{-alkanes}}$ record as originally intended, it did provide useful data on climate factors affecting precipitation in the Laguna Saladilla region. The semi-inverse relationship between the δ^2H_{Bulk} and $\delta^2H_{n\text{-alkanes}}$ record,

especially during times of more extreme climate change like the TCD, illustrate that the δ^2H_{Bulk} is also showing changes in precipitation, even if not in the same manner as the $\delta^2H_{n\text{-alkanes}}$record. The comparison of δ^2H_{Bulk} and $\delta^2H_{n\text{-alkanes}}$ isotopes in this study provides evidence supporting research that the δ^2H_{Bulk} proxy provides data on precipitation source rather than precipitation amount in some cases (Araguás-Araguás and Diaz Teijeiro, 2005).

Furthermore, as the use of δ^2H_{Bulk} isotopes for the reconstruction of paleoenvironments is an emerging proxy, the correlation of the acidified and non-acidified samples in this study provide data to contribute to future use of this proxy. My results indicate that either acidified or nonacidified samples can be used for δ^2H_{Bulk} analysis.

The proxy data from my thesis research illuminate some of the diverse climate drivers across the Caribbean that may be more responsible for precipitation in the northwestern coastal region of Hispaniola. The δ^2H_{Bulk} data presented here provide a record of times with increased convective activity in the region leading to more overall precipitation and decreased E/P ratios. While precipitation at Laguna Saladilla is mainly affected by polar outbreaks in the north, climate drivers bringing more convective activity to the area can cause increased precipitation in this usually dry region. Future work on this research will be needed to better understand the organic matter source of hydrogen isotope composition in the δ^2H_{Bulk} record to fully understand how it relates to the other proxies in the study.

REFERENCES

Abbott, R.T., 1954. American seashells. D. van Nostrand Company, Princeton, New Jersey.

Abbott, R.T., Morris, P.A., 1995. A field guide to shells; Atlantic and Gulf Coasts and the West Indies. The Peterson Field Guide Series 4th ed. Houghton Mifflin, Boston, Massachusetts.

Anchukaitis, K.J. and Horn, S.P., 2005. A 2000-year reconstruction of forest disturbance from southern Pacific Costa Rica. *Palaeogeography, Palaeoclimatology, Palaeoecology*, *221*(1–2), pp.35–54.

Angeles, M.E., Gonzalez, J.E., Ramírez-Beltrán, N.D., Tepley, C.A. and Comarazamy, D.E., 2010. Origins of the Caribbean rainfall bimodal behavior. *Journal of Geophysical Research: Atmospheres*, *115*(D11).

Araguás-Araguás, L.J. and Diaz Teijeiro, M.F., 2005. Isotope composition of precipitation and water vapour in the Iberian Peninsula: first results of the Spanish network of isotopes in precipitation. *International Atomic Energy Agency Technical Report*, *1453*, pp.173–190.

Baker, P.A., Seltzer, G.O., Fritz, S.C., Dunbar, R.B., Grove, M.J., Tapia, P.M., Cross, S.L., Rowe, H.D. and Broda, J.P., 2001. The history of South American tropical precipitation for the past 25,000 years. *Science*, *291*(5504), pp.640–643.

Beets, C.J., Troelstra, S.R., Grootes, P.M., Nadeau, M.J., Borg, K.V., de Jong, A.F., Hofman, C.L. and Hoogland, M.L., 2006. Climate and pre-Columbian settlement at Anse à la Gourde, Guadeloupe, Northeastern Caribbean. *Geoarchaeology*, *21*(3), pp.271–280.

Bender, M.M., 1971. Variations in the 13C/12C ratios of plants in relation to the pathway of photosynthetic carbon dioxide fixation. *Phytochemistry 10*, 1239–1244.

Bhattacharya, T., Chiang, J.C. and Cheng, W., 2017. Ocean-atmosphere dynamics linked to 800–1050 CE drying in mesoamerica. *Quaternary Science Reviews*, *169*, pp.263–277.

Blaauw, M and Christen, J.A. 2018. rbacon: Age-Depth Modelling using Bayesian Statistics. R package version 2.3.4.

Bolay, E., 1997. The Dominican Republic: a country between rain forest and desert. Contributions to the ecology of a Caribbean island. Margraf Verlag, Weikersheim, Germany.

Burn, M.J. and Palmer, S.E., 2014. Solar forcing of Caribbean drought events during the last millennium. *Journal of Quaternary Science*, *29*(8), pp.827–836.

Burn, M.J., Holmes, J., Kennedy, L.M., Bain, A., Marshall, J.D. and Perdikaris, S., 2016. A sediment-based reconstruction of Caribbean effective precipitation during the 'Little Ice Age'from Freshwater Pond, Barbuda. *The Holocene*, *26*(8), pp.1237–1247.

Caffrey, M.A., 2011. Holocene climate and environmental history of Laguna Saladilla, Dominican Republic. PhD. Dissertation, University of Tennessee, Knoxville.

Caffrey, M.A. and Horn, S.P., 2015. Long-term fire trends in Hispaniola and Puerto Rico from sedimentary charcoal: a comparison of three records. *Professional Geographer, 67(2)*, pp. 229-241.

Caffrey, M.A., Horn, S.P., Orvis, K.H. and Haberyan, K.A., 2015. Holocene environmental change at Laguna Saladilla, coastal north Hispaniola. *Palaeogeography, Palaeoclimatology, Palaeoecology*, *436*, pp.9–22.

Chen, A. and Taylor, M.A., 2002. Investigating the link between early season Caribbean rainfall and the El Niño+ 1 year. *International Journal of Climatology*, *22*(1), pp.87–106.

Clark, J.S., 1990. Fire and climate change during the last 750 yr in northwestern Minnesota. *Ecological Monographs*, *60*(2), pp.135–159.

Clark, R., 1982. Point count estimation of charcoal in pollen preparations and thin sections of sediments. Pollen Spores 24, pp.523–535.

Clement, R.M. and Horn, S.P., 2001. Pre-Columbian land-use history in Costa Rica: a 3000-year record of forest clearance, agriculture and fires from Laguna Zoncho. *The Holocene*, *11*(4), pp.419–426.

Colinvaux, P., De Oliveira, P.E., Moreno, P., 1999. Amazon Pollen Manual and Atlas. Harwood Academic Publishers, Amsterdam, The Netherlands.

Cook, K.H. and Vizy, E.K., 2010. Hydrodynamics of the Caribbean low-level jet and its relationship to precipitation. *Journal of Climate*, *23*(6), pp.1477–1494.

Crausbay, S.D., Martin, P.H. and Kelly, E.F., 2015. Tropical montane vegetation dynamics near the upper cloud belt strongly associated with a shifting ITCZ and fire. *Journal of Ecology*, *103*(4), pp.891–903.

Curtis, J.H., Hodell, D.A., Brenner, M., 1996. Climate variability on the Yucatan Peninsula (Mexico) during the past 3500 years, and implications for Maya cultural evolution. *Quaternary Research 46*, pp.37–47.

Curtis, S., 2002. Interannual variability of the bimodal distribution of summertime rainfall over Central America and tropical storm activity in the far-eastern Pacific. *Climate Research*, *22*(2), pp.141–146.

Curtis, S. and Gamble, D.W., 2008. Regional variations of the Caribbean mid-summer drought. *Theoretical and Applied Climatology*, *94*(1–2), pp.25–34.

Curtis, S. and Gamble, D.W., 2016. The boreal winter Madden-Julian Oscillation's influence on summertime precipitation in the greater Caribbean. *Journal of Geophysical Research: Atmospheres*, *121*(13), pp.7592–7605.

Dean, W.E., 1974. Determination of carbonate and organic matter in calcareous sediments and sedimentary rocks by loss on ignition: comparison with other methods. *Journal of Sedimentary Petrology 44*, pp.242–248.

Diefendorf, A.F., Mueller, K.E., Wing, S.L., Koch, P.L. and Freeman, K.H., 2010. Global patterns in leaf 13C discrimination and implications for studies of past and future climate. *Proceedings of the National Academy of Sciences*, *107*(13), pp.5738–5743.

Donnelly, J.P. and Woodruff, J.D., 2007. Intense hurricane activity over the past 5,000 years controlled by El Niño and the West African monsoon. *Nature*, *447*(7143), pp.465–468.

Douglas, P.M., Pagani, M., Brenner, M., Hodell, D.A. and Curtis, J.H., 2012. Aridity and vegetation composition are important determinants of leaf-wax δD values in southeastern Mexico and Central America. *Geochimica et Cosmochimica Acta*, *97*, pp.24–45.

Enfield, D.B. and Alfaro, E.J., 1999. The dependence of Caribbean rainfall on the interaction of the tropical Atlantic and Pacific Oceans. *Journal of Climate*, *12*(7), pp.2093–2103.

Faegri, K., Iversen, J., Kaland, P.E. and Krzywinski, K., 1989. Textbook of pollen analysis. Caldwell.Fedorov, A.V. and Philander, S.G., 2000. Is El Niño changing?. *Science*, *288*(5473), pp.1997–2002.

Fensterer, C., Scholz, D., Hoffmann, D.L., Spötl, C., Schröder-Ritzrau, A., Horn, C., Pajón, J.M. and Mangini, A., 2013. Millennial-scale climate variability during the last 12.5 ka recorded in a Caribbean speleothem. *Earth and Planetary Science Letters*, *361*, pp.143–151.

French, C. D., and Schenk, C. J. 2004. Map showing geology, oil and gas fields, and geologic provinces of the Caribbean region. US Geological Survey, Central Energy Resources Team.

Fritz, S.C., Björck, S., Rigsby, C.A., Baker, P.A., Calder-Church, A. and Conley, D.J., 2011. Caribbean hydrological variability during the Holocene as reconstructed from crater lakes on the island of Grenada. *Journal of Quaternary Science*, *26*(8), pp.829–838.

Gamble, D.W. and Curtis, S., 2008. Caribbean precipitation: review, model and prospect. *Progress in Physical Geography*, *32*(3), pp.265–276

Gamble, D.W., Parnell, D.B. and Curtis, S., 2008. Spatial variability of the Caribbean mid-summer drought and relation to north Atlantic high circulation. *International Journal of Climatology*, *28*(3), pp.343–350.

Giannini, A., Kushnir, Y. and Cane, M.A., 2000. Interannual variability of Caribbean rainfall, ENSO, and the Atlantic Ocean. *Journal of Climate*, *13*(2), pp.297–311.

Giannini, A., Cane, M.A. and Kushnir, Y., 2001a. Interdecadal changes in the ENSO teleconnection to the Caribbean region and the North Atlantic Oscillation. *Journal of Climate*, *14*(13), pp.2867–2879.

Giannini, A., Chiang, J.C., Cane, M.A., Kushnir, Y. and Seager, R., 2001b. The ENSO teleconnection to the tropical Atlantic Ocean: Contributions of the remote and local SSTs to rainfall variability in the tropical Americas. *Journal of Climate*, *14*(24), pp.4530–4544.

Goman, M. and Byrne, R., 1998. A 5000-year record of agriculture and tropical forest clearance in the Tuxtlas, Veracruz, Mexico. *The Holocene*, *8*(1), pp.83–89.

Granger, O.E., 1985. Caribbean climates. *Progress in Physical Geography*, *9*(1), pp.16–43.

Griffiths, J.F. and Driscoll, D.M., 1982. *Survey of climatology*. Merrill Publishing Company.

Hassan, K.M. and Spalding, R.F., 2001. Hydrogen isotope values in lacustrine kerogen. *Chemical Geology*, *175*(3–4), pp.713–721.

Hastenrath, S.L., 1967. Rainfall distribution and regime in Central America. *Archiv für Meteorologie, Geophysik und Bioklimatologie, Serie B*, *15*(3), pp.201–241.

Hastenrath, S., 1976. Variations in low-latitude circulation and extreme climatic events in the tropical Americas. *Journal of the Atmospheric Sciences*, *33*(2), pp.202–215.

Hastenrath, S., 1978. On modes of tropical circulation and climate anomalies. *Journal of the Atmospheric Sciences*, *35*(12), pp.2222–2231.

Hastenrath, S., 1984. Interannual variability and annual cycle: Mechanisms of circulation and climate in the tropical Atlantic sector. *Monthly Weather Review*, *112*(6), pp.1097–1107.

Haug, G.H., Hughen, K.A., Sigman, D.M., Peterson, L.C. and Röhl, U., 2001. Southward migration of the intertropical convergence zone through the Holocene. *Science*, *293*(5533), pp.1304–1308.

Haug, G.H., Günther, D., Peterson, L.C., Sigman, D.M., Hughen, K.A. and Aeschlimann, B., 2003. Climate and the collapse of Maya civilization. *Science*, *299*(5613), pp.1731–1735.

Higuera-Gundy, A., Brenner, M., Hodell, D.A., Curtis, J.H., Leyden, B.W. and Binford, M.W., 1999. A 10,300 14 C yr record of climate and vegetation change from Haiti. *Quaternary Research*, *52*(2), pp.159–170.

Hodell, D.A., Curtis, J.H., Jones, G.A., Higuera-Gundy, A., Brenner, M., Binford, M.W. and Dorsey, K.T., 1991. Reconstruction of Caribbean climate change over the past 10,500 years. *Nature*, *352*(6338), pp.790–793.

Hodell, D.A., Brenner, M. and Curtis, J.H., 2005. Terminal Classic drought in the northern Maya lowlands inferred from multiple sediment cores in Lake Chichancanab (Mexico). *Quaternary Science Reviews*, *24*(12–13), pp.1413–1427.

Horn, S.P., and Sanford Jr., R.L., 1992. Holocene fires in Costa Rica. *Biotropica 24*, pp.354–361.

Horn, S.P., 1993. Postglacial vegetation and fire history in the Chirripó páramo of Costa Rica. *Quaternary Research 40,* pp.107–116.

Hou, J., D'Andrea, W.J. and Huang, Y., 2008. Can sedimentary leaf waxes record D/H ratios of continental precipitation? Field, model, and experimental assessments. *Geochimica et Cosmochimica Acta*, *72*(14), pp.3503–3517.

IPCC, 2007: Climate Change 2007: The Physical Science Basis. Contribution of Working Group I to the Fourth Assessment Report of the Intergovernmental Panel on Climate Change [Solomon, S., D. Qin, M. Manning, Z. Chen, M. Marquis, K.B. Averyt, M.Tignor and H.L. Miller (eds.)]. Cambridge University Press, Cambridge, United Kingdom and New York, NY, USA.

Juggins, S., 2007. C2 version 1.5 user guide: software for ecological and palaeoecological data analysis and visualization. Newcastle University, Newcastle upon Tyne, UK

Jury, M., Malmgren, B.A. and Winter, A., 2007. Subregional precipitation climate of the Caribbean and relationships with ENSO and NAO. *Journal of Geophysical Research: Atmospheres*, *112*(D16).

Kennedy, L.M., Horn, S.P. and Orvis, K.H., 2006. A 4000-year record of fire and forest history from Valle de Bao, Cordillera Central, Dominican Republic. *Palaeogeography, Palaeoclimatology, Palaeoecology*, *231*(3–4), pp.279–290.

Kennett, D.J., Breitenbach, S.F., Aquino, V.V., Asmerom, Y., Awe, J., Baldini, J.U., Bartlein, P., Culleton, B.J., Ebert, C., Jazwa, C. and Macri, M.J., 2012. Development and disintegration of Maya political systems in response to climate change. *Science*, *338*(6108), pp.788–791.

Kohn, M.J., 2010. Carbon isotope compositions of terrestrial C3 plants as indicators of (paleo) ecology and (paleo) climate. *Proceedings of the National Academy of Sciences*, *107*(46), pp.19691–19695.

Krishnamurthy, R.V., Syrup, K.A., Baskaran, M. and Long, A., 1995. Late glacial climate record of midwestern United States from the hydrogen isotope ratio of lake organic matter. *Science*, *269*(5230), pp.1565–1567.

Lachniet, M.S., Burns, S.J., Piperno, D.R., Asmerom, Y., Polyak, V.J., Moy, C.M. and Christenson, K., 2004. A 1500-year El Niño/Southern Oscillation and rainfall history for the isthmus of Panama from speleothem calcite. *Journal of Geophysical Research: Atmospheres*, *109*(D20).

Lafon, C.W., Naito, A.T., Grissino-Mayer, H.D., Horn, S.P. and Waldrop, T.A., 2017. Fire history of the Appalachian region: a review and synthesis. General Technical Report SRS-219. Asheville, North Carolina: U.S. Department of Agriculture, Forest Service, Southern Research Station. 97 p.

Lane, C.S. and Horn, S.P., 2013. Terrestrially derived n-alkane δD evidence of shifting Holocene paleohydrology in highland Costa Rica. *Arctic, antarctic, and alpine research*, *45*(3), pp.342–349.

Lane, C.S., Horn, S.P. and Kerr, M.T., 2014. Beyond the Mayan lowlands: impacts of the terminal classic drought in the Caribbean Antilles. *Quaternary Science Reviews*, *86*, pp.89–98.

Lane, C.S., Horn, S.P., and Mora, C.I., 2004. Stable carbon isotope ratios in lake and swamp sediments as proxies for prehistoric forest clearance and crop cultivation in the Neotropics. *Journal of Paleolimnology* 32, pp.375–381.

Lane, C.S., Horn, S.P., Mora, C.I. and Orvis, K.H., 2009. Late-Holocene paleoenvironmental change at mid-elevation on the Caribbean slope of the Cordillera Central, Dominican Republic: a multi-site, multi-proxy analysis. *Quaternary Science Reviews*, *28*(23–24), pp.2239–2260.

Lane, C.S., Horn, S.P., Orvis, K.H. and Thomason, J.M., 2011. Oxygen isotope evidence of Little Ice Age aridity on the Caribbean slope of the Cordillera Central, Dominican Republic. *Quaternary Research*, *75*(3), pp.461–470.

LeBlanc, A.R., Kennedy, L.M., Liu, K.B. and Lane, C.S., 2017. Linking hurricane landfalls, precipitation variability, fires, and vegetation response over the past millennium from analysis of coastal lagoon sediments, southwestern Dominican Republic. *Journal of Paleolimnology*, *58*(2), pp.135–150.

Linsley, B.K., Dunbar, R.B., Wellington, G.M. and Mucciarone, D.A., 1994. A coral-based reconstruction of Intertropical Convergence Zone variability over Central America since 1707. *Journal of Geophysical Research: Oceans*, *99*(C5), pp.9977–9994.

Lovan, N.A. and Krishnamurthy, R.V., 2011. Inferring paleotemperature from the D/H ratio of lacustrine organic matter. *Quaternary international*, *229*(1–2), pp.38–46.

Magaña, V., Amador, J.A. and Medina, S., 1999. The midsummer drought over Mexico and Central America. *Journal of Climate*, *12*(6), pp.1577–1588.

Mangini, A., Blumbach, P., Verdes, P., Spötl, C., Scholz, D., Machel, H. and Mahon, S., 2007. Combined records from a stalagmite from Barbados and from lake sediments in Haiti reveal variable seasonality in the Caribbean between 6.7 and 3 ka BP. *Quaternary Science Reviews*, *26*(9–10), pp.1332–1343.

Mann, M.E., Zhang, Z., Rutherford, S., Bradley, R.S., Hughes, M.K., Shindell, D., Ammann, C., Faluvegi, C., Ni, F., 2009. Global signatures and dynamical origins of the Little Ice Age and Medieval Climate Anomaly. *Science 326*, pp.1256–1260.

Mapes, B.E., Liu, P. and Buenning, N., 2005. Indian monsoon onset and the Americas midsummer drought: Out-of-equilibrium responses to smooth seasonal forcing. *Journal of climate*, *18*(7), pp.1109–1115.

Martin, E.R. and Schumacher, C., 2011. Modulation of Caribbean precipitation by the Madden–Julian oscillation. *Journal of Climate*, *24*(3), pp.813–824.

Meybeck, M., 1982. Carbon, nitrogen, and phosphorus transport by world rivers. *American Journal of Science 282*, 401–450.

Nyberg, J., Kuijpers, A., Malmgren, B.A. and Kunzendorf, H., 2001. Late Holocene changes in precipitation and hydrography recorded in marine sediments from the northeastern Caribbean Sea. *Quaternary Research*, *56*(1), pp.87–102.

Nyberg, J., Malmgren, B.A., Kuijpers, A. and Winter, A., 2002. A centennial-scale variability of tropical North Atlantic surface hydrography during the late Holocene. *Palaeogeography, Palaeoclimatology, Palaeoecology*, *183*(1–2), pp.25–41.

Peterson, L.C. and Haug, G.H., 2006. Variability in the mean latitude of the Atlantic Intertropical Convergence Zone as recorded by riverine input of sediments to the Cariaco Basin (Venezuela). *Palaeogeography, Palaeoclimatology, Palaeoecology*, *234*(1), pp.97–113.

Polissar, P.J. and D'Andrea, W.J., 2014. Uncertainty in paleohydrologic reconstructions from molecular δD values. *Geochimica et Cosmochimica Acta*, *129*, pp.146–156.

Rajendrudu, G., Prasad, J.S. and Das, V.R., 1986. C3-C4 intermediate species in Alternanthera (Amaranthaceae): leaf anatomy, CO2 compensation point, net CO2 exchange and activities of photosynthetic enzymes. *Plant Physiology*, *80*(2), pp.409–414.

Reimer, P.J., Bard, E., Bayliss, A., et al., 2013. INTCAL13 and MARINE13 radiocarbon age calibration curves 0–50,000 years cal BP. Radiocarbon 55, pp.1869–1887.

Renberg, I., 1990. A procedure for preparing large sets of diatom slides from sediment cores. *Journal of Paleolimnology. 4*, pp.87–90.

R Core Team. 2017. R: A language and environment for statistical computing. R Foundation for Statistical Computing, Vienna, Austria.

Risi, C., Bony, S. and Vimeux, F., 2008. Influence of convective processes on the isotopic composition (δ18O and δD) of precipitation and water vapor in the tropics: 2. Physical interpretation of the amount effect. *Journal of Geophysical Research: Atmospheres*, *113*(D19).

Sachs, J.P., Sachse, D., Smittenberg, R.H., Zhang, Z., Battisti, D.S. and Golubic, S., 2009. Southward movement of the Pacific intertropical convergence zone AD 1400–1850. *Nature Geoscience*, *2*(7), pp.519–525.

Sachse, D., Billault, I., Bowen, G.J., Chikaraishi, Y., Dawson, T.E., Feakins, S.J., Freeman, K.H., Magill, C.R., McInerney, F.A., Van Der Meer, M.T. and Polissar, P., 2012. Molecular paleohydrology: interpreting the hydrogen-isotopic composition of lipid biomarkers from photosynthesizing organisms. *Annual Review of Earth and Planetary Sciences*, *40*, pp.221–249.

Sachse, D., Radke, J. and Gleixner, G., 2004. Hydrogen isotope ratios of recent lacustrine sedimentary n-alkanes record modern climate variability. *Geochimica et Cosmochimica Acta*, *68*(23), pp.4877–4889.

Sauer, P.E., Eglinton, T.I., Hayes, J.M., Schimmelmann, A. and Sessions, A.L., 2001. Compound-specific D/H ratios of lipid biomarkers from sediments as a proxy for environmental and climatic conditions1. *Geochimica et Cosmochimica Acta*, *65*(2), pp.213–222.

Sauer, P.E., Schimmelmann, A., Sessions, A.L. and Topalov, K., 2009. Simplified batch equilibration for D/H determination of non-exchangeable hydrogen in solid organic material. *Rapid communications in mass spectrometry*, *23*(7), pp.949–956.

Schefuss, E., Kuhlmann, H., Mollenhauer, G., Prange, M. and Pätzold, J., 2011. Forcing of wet phases in southeast Africa over the past 17,000 years. *Nature*, *480*(7378), pp.509–512.

Schimmelmann, A., Lewan, M.D. and Wintsch, R.P., 1999. D/H isotope ratios of kerogen, bitumen, oil, and water in hydrous pyrolysis of source rocks containing kerogen types I, II, IIS, and III. *Geochimica et Cosmochimica Acta*, *63*(22), pp.3751–3766.

Schneider, T., Bischoff, T. and Haug, G.H., 2014. Migrations and dynamics of the intertropical convergence zone. *Nature*, *513*(7516), pp.45–53.

Sharpe, Z., 2007. Principles of isotope geochemistry. Pearson, Upper Saddle River, New Jersey.

Singh, B., 1997. Climate changes in the greater and southern Caribbean. *International Journal of Climatology*, *17*(10), pp.1093–1114.

Spence, J.M., Taylor, M.A. and Chen, A.A., 2004. The effect of concurrent sea-surface temperature anomalies in the tropical Pacific and Atlantic on Caribbean rainfall. *International Journal of Climatology*, *24*(12), pp.1531–1541.

Stuiver, M., and Reimer, P.J., 1993. Extended 14C database and revised CALIB 3.0 14C age calibration program. Radiocarbon 35, pp.215–230.

Sutton, R.T. and Hodson, D.L., 2005. Atlantic Ocean forcing of North American and European summer climate. *Science*, *309*(5731), pp.115–118.

Talbot, M.R., 2001. Nitrogen isotopes in paleolimnology. In: Last, W.M., and Smol, J.P. (Eds.), Tracking Environmental Change Using Lake Sediments. Volume 2: Physical and Geochemical Methods. Kluwer Academic Publishers, Dordrecht, The Netherlands, pp. 401–439.

Taylor, M.A., Enfield, D.B. and Chen, A.A., 2002. Influence of the tropical Atlantic versus the tropical Pacific on Caribbean rainfall. *Journal of Geophysical Research: Oceans*, *107*(C9).

Ting, M., Kushnir, Y., Seager, R. and Li, C., 2009. Forced and internal twentieth-century SST trends in the North Atlantic. *Journal of Climate*, *22*(6), pp.1469–1481.

Wang, C., 2007. Variability of the Caribbean low-level jet and its relations to climate. *Climate Dynamics*, *29*(4), pp.411–422.

Webster, J.W., Brook, G.A., Railsback, L.B., Cheng, H., Edwards, R.L., Alexander, C., Reeder, P.P., 2007. Stalagmite evidence from Belize indicating significant droughts at the time of Preclassic abandonment, the Maya Hiatus, and the Classic Maya collapse. *Palaeogeography Palaeoclimatology Palaeoecology 250*, pp.1–17.

Whitlock, C. and Larsen, C., 2001. Charcoal as a fire proxy. In Smol, JP, Birks, HJB and Last, WM., editors, Tracking environmental change using lake sediments. Volume 3: terrestrial, algal, and siliceous indicators. Kluwer Academic Publishers, pp.75–97.

Whitlock, C. and Anderson, R.S., 2003. Fire history reconstructions based on sediment records from lakes and wetlands. *Fire and climatic change in temperate ecosystems of the western Americas* , pp. 3–31.

Whyte, F.S., Taylor, M.A., Stephenson, T.S. and Campbell, J.D., 2008. Features of the Caribbean low level jet. *International Journal of Climatology*, *28*(1), pp.119–128.

Winter, A., Ishioroshi, H., Watanabe, T., Oba, T. and Christy, J., 2000. Caribbean Sea surface temperatures: Two-to-three degrees cooler than present during the Little Ice Age. *Geophysical Research Letters*, *27*(20), pp.3365–3368.

World Meteorological Organization (WMO), 2017. World weather information service: Montecristi [Online]

VITA

Elizabeth Marie MacLennan was born in Chattanooga, TN on March 22, 1994. She attended Girl's Preparatory School for high school, graduating in Spring of 2012. From there, Elizabeth went to college at the University of Tennessee. She graduated Summa Cum Laude in Spring of 2016 with a Bachelor of the Art's degree with a double major in Sustainability and Geography. While working under Dr. Sally Horn during her undergraduate career, she became interested in climate change and lake sediments. She chose to continue her education at the University of Tennessee to pursue a Master of Science degree in Geography.

She started the graduate program in Spring of 2017 to study the paleoclimate of Hispaniola through the use of lake sediments. While in the graduate program, Elizabeth was a research assistant to Dr. Kelsey Ellis under the NOAA VORTEX-SE project and a graduate teaching assistant, instructing laboratory courses for physical geography courses.